

# 7

## Propagated Signaling: The Action Potential

### The Action Potential Is Generated by the Flow of Ions Through Voltage-Gated Channels

Sodium and Potassium Currents Through Voltage-Gated Channels Are Recorded with the Voltage Clamp

Voltage-Gated Sodium and Potassium Conductances Are Calculated from Their Currents

The Action Potential Can Be Reconstructed from the Properties of Sodium and Potassium Channels

### Variations in the Properties of Voltage-Gated Ion Channels Expand the Signaling Capabilities of Neurons

The Nervous System Expresses a Rich Variety of Voltage-Gated Ion Channels

Gating of Voltage-Sensitive Ion Channels Can Be Influenced by Various Cytoplasmic Factors

Excitability Properties Vary Between Regions of the Neuron

Excitability Properties Vary Between Types of Neurons

### The Mechanisms of Voltage-Gating and Ion Permeation Have Been Inferred from Electrophysiological Measurements

Voltage-Gated Sodium Channels Open and Close in Response to Redistribution of Charges Within the Channel

Voltage-Gated Sodium Channels Select for Sodium on the Basis of Size, Charge, and Energy of Hydration of the Ion

### Voltage-Gated Potassium, Sodium, and Calcium Channels Stem from a Common Ancestor and Have Similar Structures

X-Ray Crystallographic Analysis of Voltage-Gated Channel Structures Provides Insight into Voltage-Gating

The Diversity of Voltage-Gated Channel Types Is Generated by Several Genetic Mechanisms

### An Overall View

**N**ERVE CELLS ARE ABLE TO CARRY electrical signals over long distances because the long-distance signal, the action potential, is continually regenerated and thus does not attenuate as it moves down the axon. In Chapter 6 we saw how an action potential arises from sequential changes in the membrane's permeability to  $\text{Na}^+$  and  $\text{K}^+$  ions. We also considered how the membrane's passive properties influence the speed at which action potentials are conducted. In this chapter we focus on the voltage-gated ion channels that are critical for generating and propagating action potentials and consider how these channels are responsible for many important features of a neuron's electrical excitability.

Action potentials have four properties important for neuronal signaling. First, they have a threshold for initiation. As we saw in Chapter 6, in many nerve cells the membrane behaves as a simple resistor in response to small hyperpolarizing or depolarizing current steps. The membrane voltage changes in a graded manner as a function of the size of the current step according to Ohm's law,  $\Delta V = \Delta I \cdot R$  (in terms of conductance,  $\Delta V = \Delta I / G$ ). However, as the size of the depolarizing current increases, eventually a threshold voltage is reached, typically at around  $-50$  mV, at which point an action potential is generated (see Figure 6-2C). Second, the action potential is an all-or-none event. The size and shape of an action potential initiated by

a large depolarizing current is the same as that of an action potential evoked by a current that just surpasses the threshold.<sup>1</sup> Third, the action potential is conducted without decrement. It has a self-regenerative feature that keeps the amplitude constant, even when it is conducted over great distances. Fourth, the action potential is followed by a refractory period. For a brief time after an action potential is generated, the neuron's ability to fire a second action potential is suppressed. The refractory period limits the frequency at which a nerve can fire action potentials, and thus limits the information-carrying capacity of the axon.

These four properties of the action potential—initiation threshold, all-or-none nature, conduction without decrement, and refractory period—are unusual for biological processes, which typically respond in a graded fashion to changes in the environment. Biologists were puzzled by these properties for almost 100 years after the action potential was first measured in the mid 1800s. Finally, in the late 1940s and early 1950s studies of the membrane properties of the giant axon of the squid by Alan Hodgkin, Andrew Huxley, and Bernard Katz provided the first quantitative insight into the mechanisms underlying the action potential.

### The Action Potential Is Generated by the Flow of Ions Through Voltage-Gated Channels

An important early insight into how action potentials are generated came from an experiment performed by Kenneth Cole and Howard Curtis. While recording from the giant axon of the squid they found that ion conductance across the membrane increases dramatically during the action potential (Figure 7–1). This discovery provided the first evidence that the action potential results from changes in the flux of ions through channels in the membrane. It also raised two central questions: Which ions are responsible for the action potential, and how is the conductance of the membrane regulated?

A key insight into this problem was provided by Alan Hodgkin and Bernard Katz, who found that the amplitude of the action potential is reduced when the external  $\text{Na}^+$  concentration is lowered, indicating that  $\text{Na}^+$  influx is responsible for the rising phase of

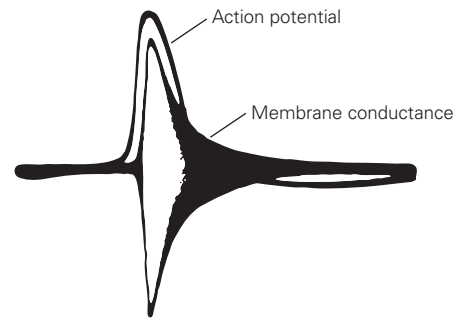


**Figure 7–1** The action potential results from an increase in ionic conductance of the axon membrane. This historic recording from an experiment conducted in 1939 by Kenneth Cole and Howard Curtis shows the oscilloscope record of an action potential superimposed on a simultaneous record of membrane conductance.

the action potential. They proposed that depolarization of the cell above threshold causes a brief increase in the cell membrane's permeability to  $\text{Na}^+$ , during which  $\text{Na}^+$  permeability overwhelms the dominant  $\text{K}^+$  permeability of the resting cell membrane, thereby driving the membrane potential towards  $E_{\text{Na}}$ . Their data also suggested that the falling phase of the action potential was caused by a later increase in  $\text{K}^+$  permeability.

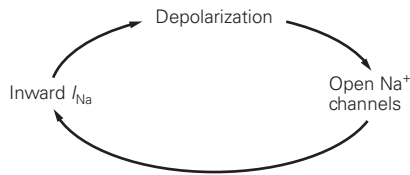
### Sodium and Potassium Currents Through Voltage-Gated Channels Are Recorded with the Voltage Clamp

This insight of Hodgkin and Katz raised a further question. What mechanism is responsible for regulating the changes in the  $\text{Na}^+$  and  $\text{K}^+$  permeabilities of the membrane? Hodgkin and Andrew Huxley reasoned that the  $\text{Na}^+$  and  $\text{K}^+$  permeabilities were regulated directly by the membrane voltage. To test this hypothesis they systematically varied the membrane potential in the squid giant axon and measured the resulting changes in the conductance of voltage-gated  $\text{Na}^+$  and  $\text{K}^+$  channels. To do this they made use of a new apparatus, the voltage clamp, developed by Kenneth Cole.

Prior to the availability of the voltage-clamp technique, attempts to measure  $\text{Na}^+$  and  $\text{K}^+$  conductance as a function of membrane potential had been limited by the strong interdependence of the membrane potential and the gating of  $\text{Na}^+$  and  $\text{K}^+$  channels. For example, if the membrane is depolarized sufficiently to open some of the voltage-gated  $\text{Na}^+$  channels, the influx of  $\text{Na}^+$  through these channels causes further depolarization. The additional depolarization causes still more

<sup>1</sup>The all-or-none property describes an action potential that is generated under a specific set of conditions. The size and shape of the action potential *can* be affected by changes in membrane properties, ion concentrations, temperature, and other variables, as discussed later in the chapter.

$\text{Na}^+$  channels to open and consequently induces more inward  $\text{Na}^+$  current:



This positive feedback cycle, which eventually drives the membrane potential to the peak of the action potential, makes it impossible to achieve a stable membrane potential. A similar coupling between current

and membrane potential complicates the study of the voltage-gated  $\text{K}^+$  channels.

The voltage clamp interrupts the interaction between the membrane potential and the opening and closing of voltage-gated ion channels. It does so by adding or withdrawing a current from the axon that is equal to the current flowing through the voltage-gated membrane channels. In this way the voltage clamp prevents the membrane potential from changing. The amount of current that must be generated by the voltage clamp to keep the membrane potential constant provides a direct measure of the current flowing across the membrane (Box 7-1). Using the voltage-clamp

### Box 7-1 Voltage-Clamp Technique

The voltage-clamp technique was developed by Kenneth Cole in 1949 to stabilize the membrane potential of neurons for experimental purposes. It was used by Alan Hodgkin and Andrew Huxley in the early 1950s in a series of experiments that revealed the ionic mechanisms underlying the action potential.

The voltage clamp permits the experimenter to “clamp” the membrane potential at predetermined levels, preventing changes in membrane current from influencing the membrane potential. By controlling the membrane potential one can measure the effect of changes in membrane potential on the membrane’s conductance of individual ion species.

The voltage clamp consists of one intracellular and extracellular pair of electrodes used to measure the membrane potential and one intracellular and extracellular pair of electrodes used to pass current across the membrane (Figure 7-2). Through the use of a negative feedback amplifier, the voltage clamp is able to pass the correct amount of current across the cell membrane to rapidly step the membrane to a constant predetermined potential.

Depolarization opens voltage-gated  $\text{Na}^+$  and  $\text{K}^+$  channels, initiating movement of  $\text{Na}^+$  and  $\text{K}^+$  across the membrane. This change in membrane current ordinarily would change the membrane potential, but the voltage clamp maintains the membrane potential at a predetermined (commanded) level.

When  $\text{Na}^+$  channels open in response to a moderate depolarizing voltage step, an inward ionic current develops because  $\text{Na}^+$  ions are driven through these channels by their electrochemical driving force. This  $\text{Na}^+$  influx would normally depolarize the membrane by increasing the positive charge on the inside of the membrane and reducing the positive charge on the outside.

The voltage clamp intervenes in this process by simultaneously withdrawing positive charges from the cell and depositing them in the external solution. By generating a current that is equal and opposite to the ionic current through the membrane, the voltage-clamp circuit automatically prevents the ionic current from changing the membrane potential from the commanded value. As a result, the *net* amount of charge separated by the membrane does not change and therefore no significant change in  $V_m$  can occur.

The voltage clamp is a negative feedback system. A negative feedback system is one in which the value of the output of the system ( $V_m$  in this case) is fed back as the input to a system and compared to a reference value (the command signal). Any difference between the command signal and the output signal activates a “controller” (the feedback amplifier in this case) that automatically reduces the difference. Thus the actual membrane potential automatically and precisely follows the command potential.

For example, assume that an inward  $\text{Na}^+$  current through the voltage-gated  $\text{Na}^+$  channels ordinarily causes the membrane potential to become more positive than the command potential. The input to the feedback amplifier is equal to  $(V_{\text{command}} - V_m)$ . The amplifier generates an output voltage equal to this error signal multiplied by the gain of the amplifier. Thus, both the input and the resulting output voltage at the feedback amplifier will be negative.

This negative output voltage will make the internal current electrode negative, withdrawing net positive charge from the cell through the voltage-clamp circuit. As the current flows around the circuit, an equal amount of net positive charge will be deposited into the external solution through the other current electrode.

A refinement of the voltage clamp, the patch-clamp technique, allows the functional properties of single ion channels to be analyzed (see Box 5-1).

technique, Hodgkin and Huxley provided the first complete description of the ionic mechanisms underlying the action potential.

One advantage of the voltage clamp is that it readily allows the ionic and capacitive components of membrane current to be analyzed separately. As described in Chapter 6, the membrane potential  $V_m$  is proportional to the charge  $Q_m$  on the membrane capacitance  $C_m$ . When  $V_m$  is not changing,  $Q_m$  is constant, and no capacitive current ( $\Delta Q_m / \Delta t$ ) flows. Capacitive current flows *only* when  $V_m$  is changing. Therefore when the membrane potential changes in response to a very rapid step of command potential, capacitive current flows only at

the beginning and end of the step. Because the capacitive current is essentially instantaneous, the ionic currents that subsequently flow through the voltage-gated channels can be analyzed separately.

Measurements of these ionic currents can be used to calculate the voltage and time dependence of changes in membrane conductance caused by the opening and closing of  $\text{Na}^+$  and  $\text{K}^+$  channels. This information provides insights into the properties of these two types of channels.

A typical voltage-clamp experiment starts with the membrane potential clamped at its resting value. When a 10 mV depolarizing step is applied, a very brief outward current instantaneously discharges the

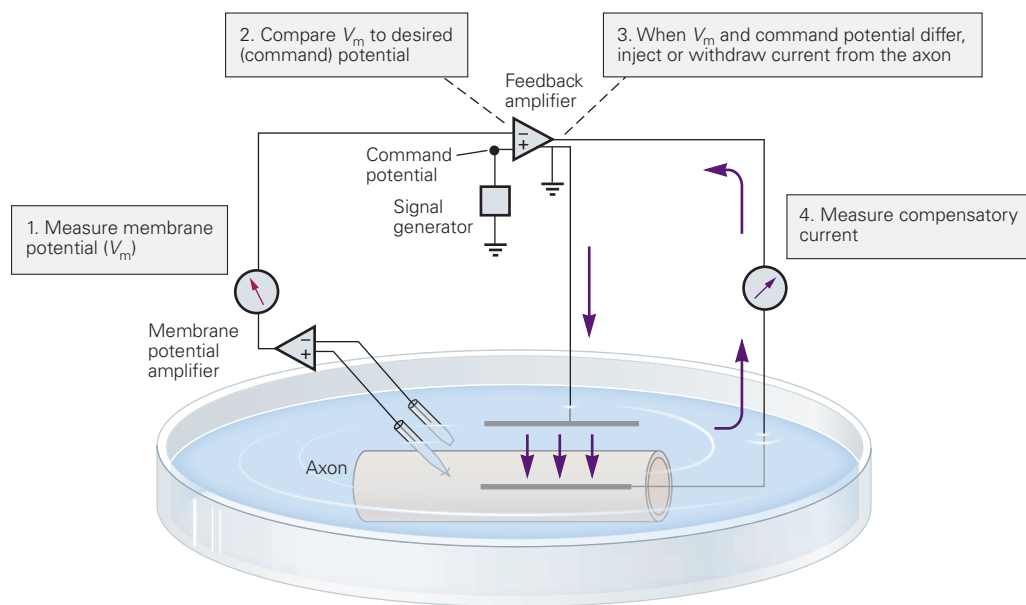


**Figure 7-2** The negative feedback mechanism of the voltage clamp. Membrane potential ( $V_m$ ) is measured by one amplifier connected to an intracellular electrode and an extracellular electrode in the bath. The membrane potential signal is displayed on an oscilloscope and is also fed into the negative terminal of the voltage-clamp feedback amplifier. The command potential, which is selected by the experimenter and can be of any desired amplitude and waveform, is fed into the positive terminal of the feedback amplifier. The feedback amplifier then subtracts the membrane potential from the command potential and amplifies any difference between these two signals. The voltage output of the amplifier is connected to the internal

current electrode, a thin wire that runs the length of the axon core. The negative feedback ensures that the voltage output of the amplifier drives a current across the resistance of the current electrode that alters the membrane voltage to minimize any difference between  $V_m$  and the command potential. To accurately measure the current-voltage relationship of the cell membrane, the membrane potential must be uniform along the entire surface of the axon. This is made possible by the highly conductive internal current electrode, which short-circuits the axoplasmic resistance, reducing axial resistance to zero (see Chapter 6). This low-resistance pathway eliminates all variations in electrical potential along the axon core.

membrane capacitance by the amount required for a 10 mV depolarization. This capacitive current ( $I_c$ ) is followed by a smaller outward current that persists for the duration of the voltage step. This steady ionic current flows through the nongated resting ion channels of the membrane, which we refer to here as *leakage channels* (see Box 6–2). The current through these channels is called the *leakage current*,  $I_l$ . The total conductance of this population of channels is called the *leakage conductance* ( $g_l$ ). At the end of the step a brief inward capacitive current repolarizes the membrane to its initial voltage and the total membrane current returns to zero (Figure 7–3A).

If a large depolarizing step is commanded, the current record is more complicated. The capacitive and leakage currents both increase in amplitude. In addition, shortly after the end of the capacitive current and the start of the leakage current, an inward (negative) current develops; it reaches a peak within a few milliseconds, declines, and gives way to an outward current. This outward current reaches a plateau that is maintained for the duration of the voltage step (Figure 7–3B).

A simple interpretation of these results is that the depolarizing voltage step sequentially turns on two types of voltage-gated channels that select for two distinct ions. One type of channel conducts ions that generate an inward current, while the other conducts ions that generate an outward current. Because these two oppositely directed currents partially overlap in time, the most difficult task in analyzing voltage-clamp experiments is to determine their separate time courses.

Hodgkin and Huxley achieved this separation by changing ions in the bathing solution. By replacing  $\text{Na}^+$  with a larger, impermeant cation (choline  $\cdot \text{H}^+$ ), they eliminated the inward  $\text{Na}^+$  current. Later, the task of separating inward and outward currents was made easier by the discovery of drugs or toxins that selectively block the different classes of voltage-gated channels (Figure 7–4). Tetrodotoxin, a poison from a certain Pacific puffer fish, blocks the voltage-gated  $\text{Na}^+$  channel with a very high potency in the nanomolar range of concentration. (Ingestion of only a few milligrams of tetrodotoxin from improperly prepared puffer fish, consumed as the Japanese sushi delicacy *fugu*, can be fatal.) The cation tetraethylammonium specifically blocks the squid axon voltage-gated  $\text{K}^+$  channel.

When tetraethylammonium is applied to the axon to block the  $\text{K}^+$  channels, the total membrane current ( $I_m$ ) consists of  $I_c$ ,  $I_l$ , and  $I_{\text{Na}}$ . The leakage conductance,  $g_l$ , is constant; it does not vary with  $V_m$  or with time. Therefore the leakage current  $I_l$  can be readily calculated and subtracted from  $I_m$ , leaving  $I_{\text{Na}}$  and  $I_c$ . Because

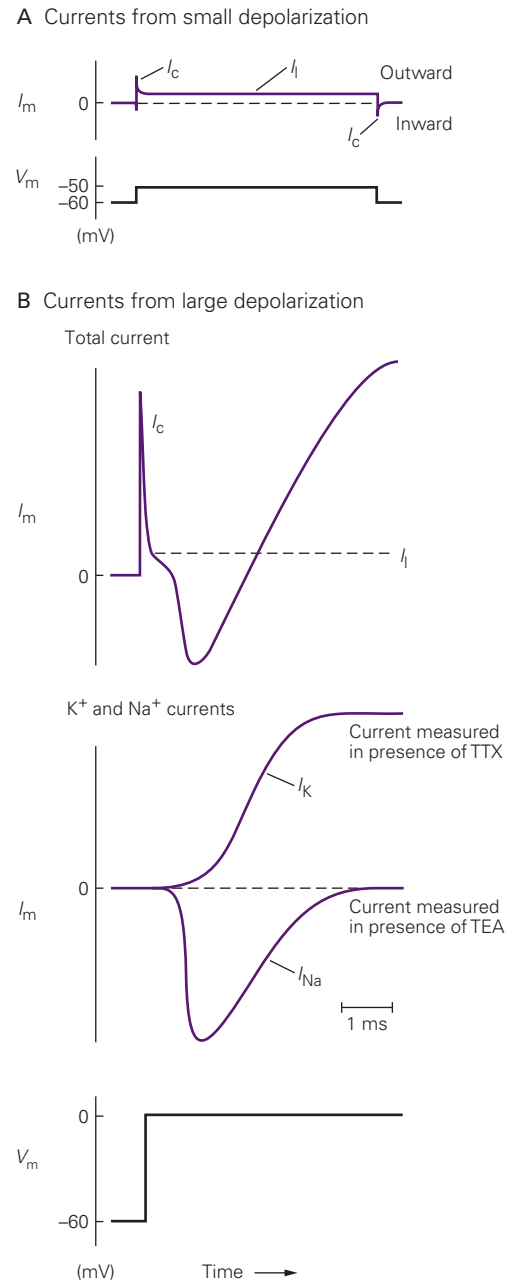


**Figure 7–3** A voltage-clamp experiment demonstrates the sequential activation of two types of voltage-gated channels.

**A.** A small depolarization (10 mV) elicits capacitive and leakage currents ( $I_c$  and  $I_l$ , respectively), the components of the total membrane current ( $I_m$ ).

**B.** A larger depolarization (60 mV) results in larger capacitive and leakage currents, plus a time-dependent inward ionic current followed by a time-dependent outward ionic current.

**Top:** Total (net) current in response to the depolarization.

**Middle:** Individual  $\text{Na}^+$  and  $\text{K}^+$  currents. Depolarizing the cell in the presence of tetrodotoxin (TTX), which blocks the  $\text{Na}^+$  current, or in the presence of tetraethylammonium (TEA), which blocks the  $\text{K}^+$  current, reveals the pure  $\text{K}^+$  and  $\text{Na}^+$  currents ( $I_K$  and  $I_{\text{Na}}$ , respectively) after subtracting  $I_c$  and  $I_l$ . **Bottom:** Voltage step.



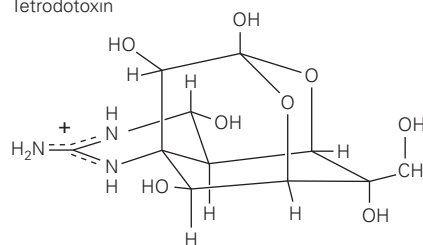
**Figure 7-4** Drugs that block voltage-gated  $\text{Na}^+$  and  $\text{K}^+$  channels.

**A.** Tetrodotoxin and saxitoxin both bind to  $\text{Na}^+$  channels with a very high affinity. Tetrodotoxin is produced by certain puffer fish, newts, and frogs. Saxitoxin is synthesized by the dinoflagellates *Gonyaulax*, which are responsible for red tides. Consumption of clams or other shellfish that have fed on the dinoflagellates during a red tide causes paralytic shellfish poisoning.

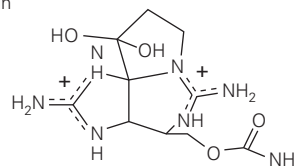
**B.** Tetraethylammonium is a cation that blocks certain voltage-gated  $\text{K}^+$  channels with a relatively low affinity. The plus signs represent positive charge. 4-Aminopyridine is another blocker of  $\text{K}^+$  channels. It is used to improve conduction of nerve impulses in patients with multiple sclerosis.

#### A $\text{Na}^+$ channel blockers

Tetrodotoxin

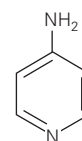


Saxitoxin

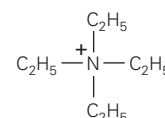


#### B $\text{K}^+$ channel blockers

4-aminopyridine



Tetraethylammonium



$I_c$  occurs only briefly at the beginning and end of the pulse, it is easily isolated by visual inspection, revealing the pure  $I_{\text{Na}}$ . Similarly,  $I_K$  can be measured when the  $\text{Na}^+$  channels are blocked by tetrodotoxin (Figure 7-3B).

By stepping the membrane to a wide range of potentials, Hodgkin and Huxley were able to measure the  $\text{Na}^+$  and  $\text{K}^+$  currents over the entire voltage extent of the action potential (Figure 7-5). They found that the  $\text{Na}^+$  and  $\text{K}^+$  currents vary as a graded function of the membrane potential. As the membrane voltage is made more positive, the outward  $\text{K}^+$  current becomes larger. The inward  $\text{Na}^+$  current also becomes larger with increases in depolarization, up to a certain extent. However, as the voltage becomes more and more positive, the  $\text{Na}^+$  current eventually declines in amplitude. When the membrane potential is +55 mV, the  $\text{Na}^+$  current is zero. Positive to +55 mV, the  $\text{Na}^+$  current reverses direction and becomes outward.

Hodgkin and Huxley explained this behavior by a very simple model in which the size of the  $\text{Na}^+$  and  $\text{K}^+$  currents is determined by two factors. The first is the magnitude of the  $\text{Na}^+$  or  $\text{K}^+$  conductance,  $g_{\text{Na}}$  or  $g_K$ , which reflects the number of  $\text{Na}^+$  or  $\text{K}^+$  channels open at any instant (see Chapter 6). The second factor is the electrochemical driving force on  $\text{Na}^+$  ions ( $V_m - E_{\text{Na}}$ ) or  $\text{K}^+$  ions ( $V_m - E_K$ ). The model is thus expressed as:

$$I_{\text{Na}} = g_{\text{Na}} \times (V_m - E_{\text{Na}})$$

$$I_K = g_K \times (V_m - E_K).$$

According to this model the amplitudes of  $I_{\text{Na}}$  and  $I_K$  change as the voltage is made more positive because there is an increase in  $g_{\text{Na}}$  and  $g_K$ . The  $\text{Na}^+$  and  $\text{K}^+$

conductances increase because the opening of the  $\text{Na}^+$  and  $\text{K}^+$  channels is voltage-dependent. The currents also change in response to changes in the electrochemical driving forces.

Both  $I_{\text{Na}}$  and  $I_K$  initially increase in amplitude as the membrane is made more positive because  $g_{\text{Na}}$  and  $g_K$  increase steeply with voltage. However, as the membrane potential approaches  $E_{\text{Na}}$  (+55 mV),  $I_{\text{Na}}$  declines because of the decrease in inward driving force, even though  $g_{\text{Na}}$  is large. That is, the positive membrane voltage now opposes the influx of  $\text{Na}^+$  down its chemical concentration gradient. At +55 mV the chemical and electrical driving forces are in balance so there is no net  $I_{\text{Na}}$ , even though  $g_{\text{Na}}$  is quite large. As the membrane is made positive to  $E_{\text{Na}}$ , the driving force on  $\text{Na}^+$  becomes positive. That is, the electrical driving force pushing  $\text{Na}^+$  out is now greater than the chemical driving force pulling  $\text{Na}^+$  in, and hence  $I_{\text{Na}}$  becomes outward. The behavior of  $I_K$  is simpler; because  $E_K$  is quite negative (−75 mV), both  $g_K$  and the outward driving force on  $\text{K}^+$  become larger as the membrane is made more positive, thereby increasing the outward  $\text{K}^+$  current.

#### Voltage-Gated Sodium and Potassium Conductances Are Calculated from Their Currents

From the two preceding equations Hodgkin and Huxley were able to calculate  $g_{\text{Na}}$  and  $g_K$  by dividing measured  $\text{Na}^+$  and  $\text{K}^+$  currents by the known  $\text{Na}^+$  and  $\text{K}^+$  electrochemical driving forces. Their results provide direct insight into how membrane voltage controls channel opening because the values of  $g_{\text{Na}}$  and  $g_K$  reflect the number of open  $\text{Na}^+$  and  $\text{K}^+$  channels (Box 7-2).

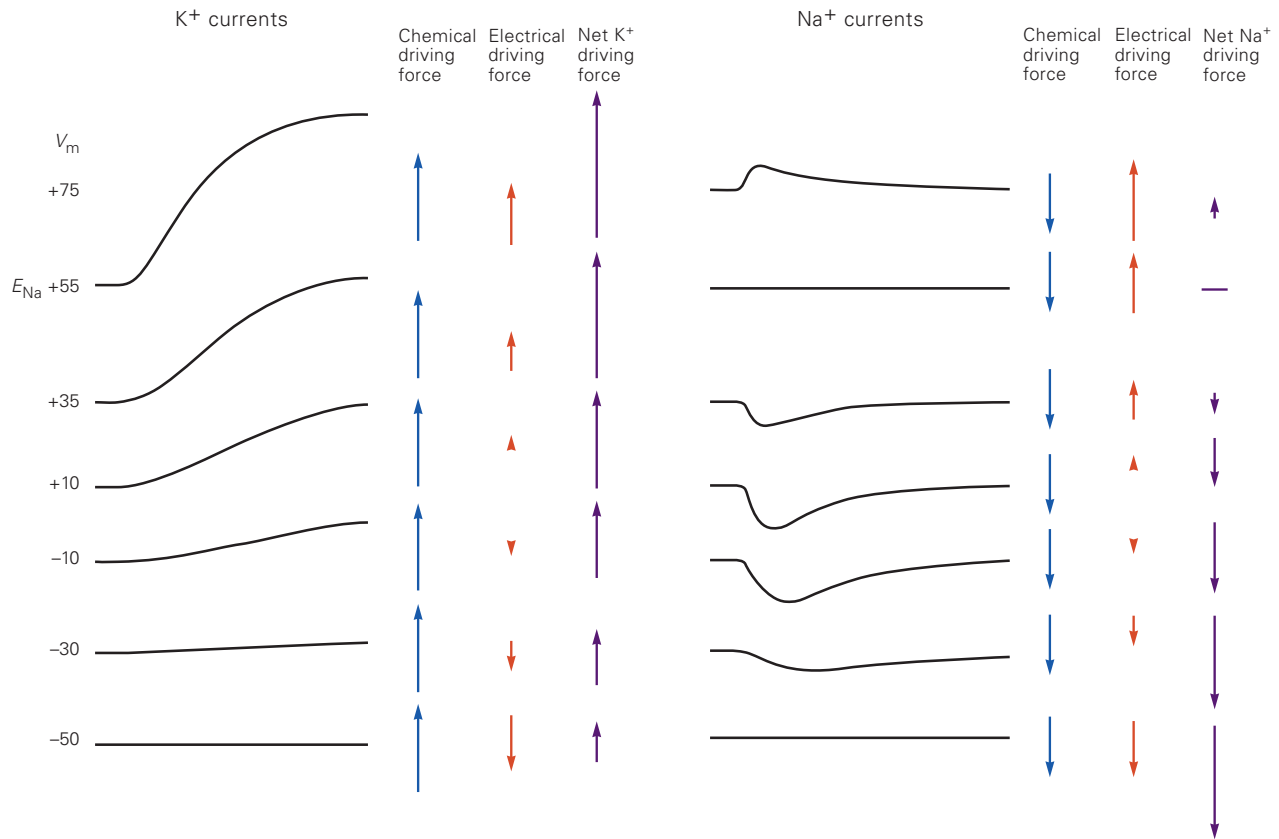


**Figure 7-5** The magnitude and polarity of the Na<sup>+</sup> and K<sup>+</sup> membrane currents vary with the amplitude of membrane depolarization. **Left:** With progressive depolarization the voltage-clamped membrane K<sup>+</sup> current increases monotonically, because both  $g_K$  and  $(V_m - E_K)$ , the driving force for K<sup>+</sup>, increase with increasing depolarization. The voltage during the depolarization is indicated at left. The direction and magnitude of the chemical ( $E_K$ ) and electrical driving force on K<sup>+</sup>, as well as the net driving force, is given by arrows at the right of each trace. (Up arrows = outward force; down arrows = inward force.)

**Right:** At first the Na<sup>+</sup> current becomes increasingly inward with increasing depolarization due to the increase in  $g_{Na}$ . However, as the membrane potential approaches  $E_{Na}$  (+55 mV) the magnitude of the inward Na<sup>+</sup> current begins to decrease due to the decrease in inward driving force ( $V_m - E_{Na}$ ). Eventually,  $I_{Na}$  goes to zero when the membrane potential reaches  $E_{Na}$ . At depolarizations positive to  $E_{Na}$ , the sign of  $(V_m - E_{Na})$  reverses, and  $I_{Na}$  becomes outward. Arrows at the right of each trace show chemical ( $E_{Na}$ ) and electrical driving forces and net Na<sup>+</sup> driving force.

Measurements of  $g_{Na}$  and  $g_K$  at various levels of membrane potential reveal two functional similarities and two differences between the Na<sup>+</sup> and K<sup>+</sup> channels. Both types of channels open in response to depolarization. Also, as the size of the depolarization increases, the probability and rate of opening increase for both types of channels. The Na<sup>+</sup> and K<sup>+</sup> channels differ, however, in the rate at which they open and in their responses to prolonged depolarization. At all levels of depolarization the Na<sup>+</sup> channels open more rapidly than K<sup>+</sup> channels (Figure 7-7). When the depolarization is maintained for some time, the Na<sup>+</sup> channels begin to close, leading to a decrease of inward current. The process by which Na<sup>+</sup> channels close during a prolonged depolarization is termed *inactivation*.

Thus depolarization causes Na<sup>+</sup> channels to switch between three different states—resting, activated, or inactivated—which represent three different conformations of the Na<sup>+</sup> channel protein (see Figure 5-7). In contrast, squid axon K<sup>+</sup> channels do not inactivate; they remain open as long as the membrane is depolarized, at least for voltage-clamp depolarizations lasting up to tens of milliseconds (Figure 7-7).

In the inactivated state the Na<sup>+</sup> channel cannot be opened by further membrane depolarization. The inactivation can be reversed only by repolarizing the membrane to its negative resting potential, whereupon the channel switches to the resting state. This switch takes some time because channels leave the inactivated state relatively slowly (Figure 7-8).

### Box 7-2 Calculation of Membrane Conductances from Voltage-Clamp Data

Membrane conductances can be calculated from voltage-clamp currents using equations derived from an equivalent circuit (Figure 7-6) that includes the membrane capacitance ( $C_m$ ); the leakage conductance ( $g_l$ ), representing the conductance of all of the resting (nongated)  $K^+$ ,  $Na^+$ , and  $Cl^-$  channels (see Chapter 6); and  $g_{Na}$  and  $g_K$ , the conductances of the voltage-gated  $Na^+$  and  $K^+$  channels.

In the equivalent circuit the ionic battery of the leakage channels,  $E_l$ , is equal to the resting membrane potential, and  $g_{Na}$  and  $g_K$  are in series with their appropriate ionic batteries.

The current through each class of voltage-gated channel may be calculated from a modified version of Ohm's law that takes into account both the electrical ( $V_m$ ) and chemical ( $E_{Na}$  or  $E_K$ ) driving forces on  $Na^+$  and  $K^+$ :

$$I_K = g_K(V_m - E_K)$$

and

$$I_{Na} = g_{Na}(V_m - E_{Na}).$$

Rearranging and solving for  $g$  gives two equations that can be used to compute the conductances of the active  $Na^+$  and  $K^+$  channel populations:

$$g_K = \frac{I_K}{(V_m - E_K)}$$

and

$$g_{Na} = \frac{I_{Na}}{(V_m - E_{Na})}.$$

In these equations the independent variable  $V_m$  is set by the experimenter. The dependent variables  $I_K$  and  $I_{Na}$  can be calculated from the records of voltage-clamp experiments (see Figure 7-5). The parameters  $E_K$  and  $E_{Na}$  can be determined empirically by finding the values of  $V_m$  at which  $I_K$  and  $I_{Na}$  reverse their polarities, that is, their *reversal potentials*.

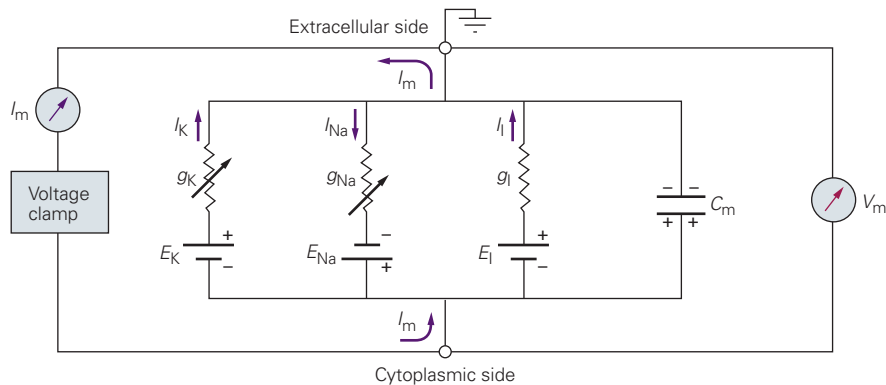


**Figure 7-6** Equivalent circuit of a voltage-clamped neuron. The voltage-gated conductance pathways ( $g_K$  and  $g_{Na}$ ) are represented by the symbol for a variable conductance—a conductor (resistor) with an arrow through it. The conductance is variable because of its dependence on time and voltage. These conductances are

in series with batteries representing the chemical gradients for  $Na^+$  and  $K^+$ . In addition there are parallel pathways for leakage current ( $g_l$  and  $E_l$ ) and capacitive current ( $C_m$ ). Arrows indicate current flow during a depolarizing step that has activated  $g_K$  and  $g_{Na}$ .

These variable, time-dependent effects of depolarization on  $g_{Na}$  are determined by the kinetics of two gating mechanisms in  $Na^+$  channels. Each  $Na^+$  channel has an *activation gate* that is closed while the membrane is at the resting potential and opened by depolarization. An *inactivation gate* is open at the resting potential and

closes after the channel opens in response to depolarization. The channel conducts  $Na^+$  only for the brief period during depolarization when *both* gates are open (Figure 7-9). Repolarization reverses the two processes, closing the activation gate and then opening the inactivation gate.



### The Action Potential Can Be Reconstructed from the Properties of Sodium and Potassium Channels

Hodgkin and Huxley were able to fit their measurements of membrane conductance to a set of empirical equations that completely describe the  $\text{Na}^+$  and  $\text{K}^+$  conductances as a function of membrane potential and time. Using these equations and measured values for the passive properties of the axon, they computed the shape and conduction velocity of the action potential.

The calculated waveform of the action potential matched the waveform recorded in the unclamped axon almost perfectly. This close agreement indicates that the mathematical model developed by Hodgkin and Huxley accurately describes the properties of the channels that are essential for generating and propagating the action potential. More than a half-century later the Hodgkin-Huxley model stands as the most successful quantitative model in neural science if not in all of biology.

According to the Hodgkin-Huxley model an action potential involves the following sequence of

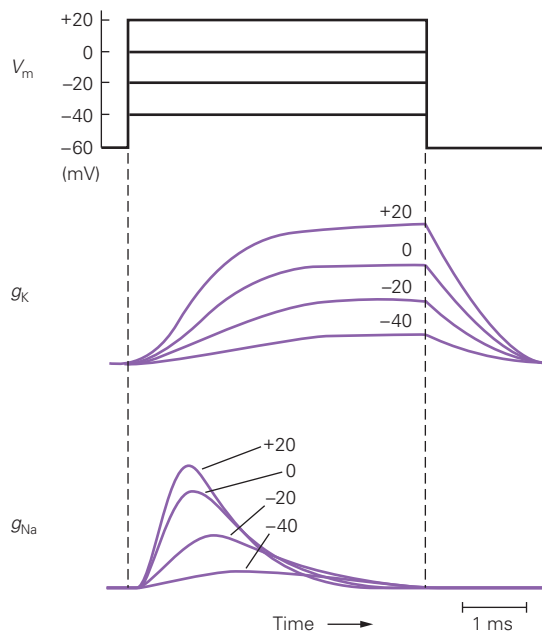


**Figure 7-7** The responses of  $\text{K}^+$  and  $\text{Na}^+$  channels to prolonged depolarization. Increasing depolarizations elicit graded increases in  $\text{K}^+$  and  $\text{Na}^+$  conductance ( $g_{\text{Na}}$  and  $g_{\text{K}}$ ), which reflect the proportional opening of thousands of voltage-gated  $\text{K}^+$  and  $\text{Na}^+$  channels. The  $\text{Na}^+$  channels open more rapidly than the  $\text{K}^+$  channels. During a maintained depolarization the  $\text{Na}^+$  channels close after opening because of the closure of an inactivation gate. The  $\text{K}^+$  channels remain open because they lack a fast inactivation process.

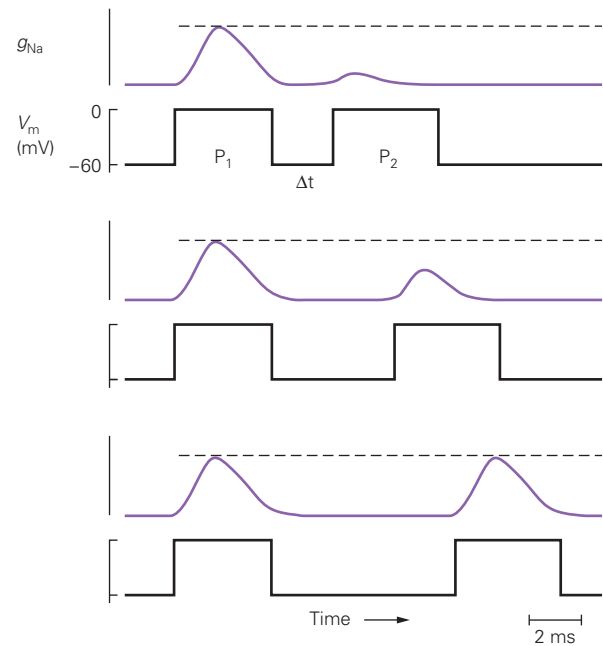
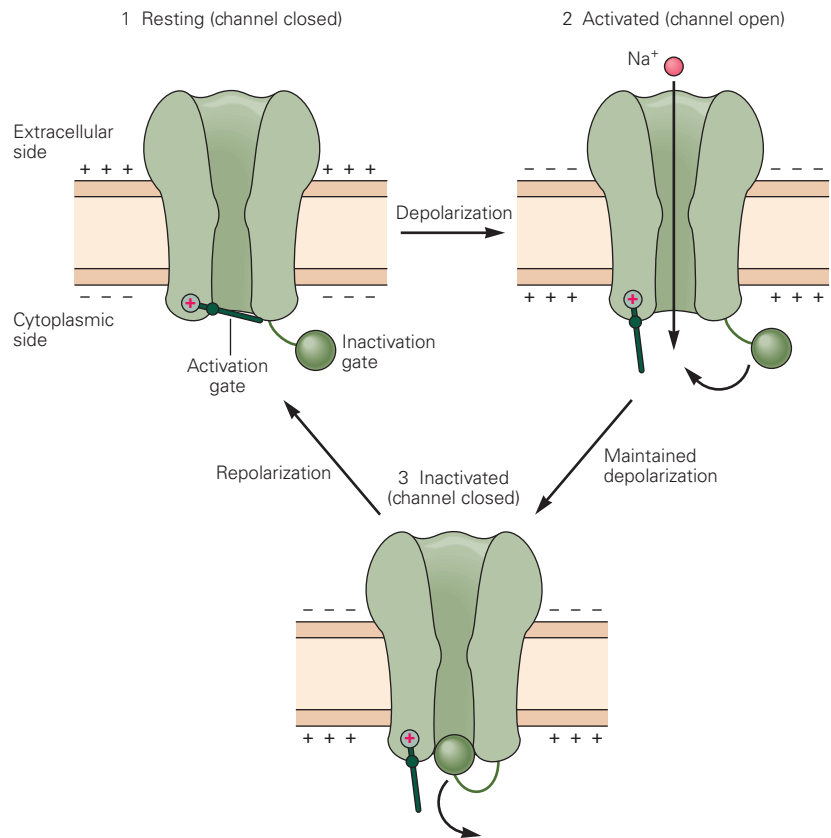


**Figure 7-8** Sodium channels remain inactivated for a few milliseconds after a depolarizing current. If the interval ( $\Delta t$ ) between two depolarizing pulses ( $P_1$  and  $P_2$ ) is brief, the second pulse produces a smaller increase in  $g_{\text{Na}}$  because many of the  $\text{Na}^+$  channels remain inactivated after the first pulse. The longer the interval between pulses, the greater the increase in  $g_{\text{Na}}$  during the second pulse, because a greater fraction of channels will have recovered from inactivation during the period of repolarization and returned to the resting state when the second pulse begins. The time course of recovery from inactivation following repolarization contributes to determining the time course of the refractory period of an action potential.

events. Depolarization of the membrane causes  $\text{Na}^+$  channels to open rapidly (an increase in  $g_{\text{Na}}$ ), resulting in an inward  $\text{Na}^+$  current. This current, by discharging the membrane capacitance, causes further depolarization, thereby opening more  $\text{Na}^+$  channels, resulting in a further increase in inward current. This regenerative process drives the membrane potential toward  $E_{\text{Na}}$ , causing the rising phase of the action potential.<sup>2</sup>

<sup>2</sup>It may at first seem inconsistent to say that current flows *outward* across the membrane when a cell is depolarized experimentally (see Figure 6-2C), while attributing the depolarization during the upstroke of the action potential to an *inward*  $\text{Na}^+$  current. However, in both cases the current across the capacitance of the membrane ( $C_m$ ) is actually outward. It is simply as a matter of convention that we describe the direction of current injected through a microelectrode as the direction in which the injected current leaves the cell across the membrane capacitance, whereas we describe the direction of the ionic membrane current as the direction of charge movement through the channels.

**Figure 7–9** Voltage-gated  $\text{Na}^+$  channels have two gates that respond in opposite ways to depolarization. In the resting state the activation gate is closed and the inactivation gate is open (1). A depolarizing stimulus results in opening of the activation gate, allowing  $\text{Na}^+$  to flow through the channel, followed by closing of the inactivation gate (2). Once the inactivation gate has closed, the channel enters the inactivated state (3). On repolarization the inactivation gate opens and the activation gate closes as the channel returns to the resting state (1). The channel is only open during the brief period when both the activation and inactivation gates are open (2).



The depolarization limits the duration of the action potential in two ways: (1) It gradually inactivates the voltage-gated  $\text{Na}^+$  channels, thus reducing  $g_{\text{Na}}$ , and (2) it opens, with some delay, the voltage-gated  $\text{K}^+$  channels, thereby increasing  $g_{\text{K}}$ . Consequently, the inward  $\text{Na}^+$  current is followed by an outward  $\text{K}^+$  current that tends to repolarize the membrane (Figure 7–10).

In most nerve cells the action potential is followed by a hyperpolarizing *after-potential*, a transient shift of the membrane potential to values more negative than the resting potential. This brief negative change in  $V_m$  occurs because the  $\text{K}^+$  channels that open during the repolarizing phase of the action potential remain open for some time after  $V_m$  has returned to its resting value. It takes a few milliseconds for all of the  $\text{K}^+$  channels to return to the closed state. During this time, when the permeability of the membrane to  $\text{K}^+$  is greater than during the resting state,  $V_m$  is slightly greater (more negative) than its normal resting value, resulting in a  $V_m$  closer to  $E_{\text{K}}$  (Figure 7–10).

The combined effect of this transient increase in  $\text{K}^+$  conductance and the residual inactivation of the  $\text{Na}^+$  channels (see Figure 7–10) underlies the *absolute*

*refractory period*, the brief period of time following an action potential when it is impossible to elicit another action potential. As some  $\text{K}^+$  channels begin to close and some  $\text{Na}^+$  channels recover from inactivation, the membrane enters the *relative refractory period*, during which it is possible to trigger an action potential, but only by applying stimuli that are stronger than those normally required to reach threshold. Together, these refractory periods typically last just 5–10 ms.

Two features of the action potential predicted by the Hodgkin-Huxley model are its threshold and all-or-none behavior. A fraction of a millivolt can be the difference between a subthreshold stimulus and a stimulus that generates a full-sized action potential. This all-or-none phenomenon may seem surprising when one considers that  $g_{\text{Na}}$  increases in a strictly *graded* manner as depolarization increases (see Figure 7–7). Each increment of depolarization increases the number of voltage-gated  $\text{Na}^+$  channels that open, thereby gradually increasing  $I_{\text{Na}}$ . How then can there be a discrete threshold for generating an action potential?

Although a small subthreshold depolarization increases the inward  $I_{\text{Na}}$ , it also increases two *outward*

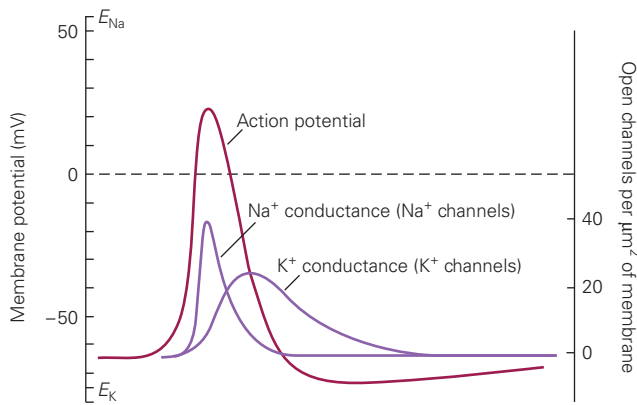


**Figure 7-10** The sequential opening of voltage-gated  $\text{Na}^+$  and  $\text{K}^+$  channels generates the action potential. One of Hodgkin and Huxley's great achievements was to dissect the change in conductance during an action potential into separate components attributable to the opening of  $\text{Na}^+$  and  $\text{K}^+$  channels. The shape of the action potential and the underlying conductance changes can be calculated from the properties of the voltage-gated  $\text{Na}^+$  and  $\text{K}^+$  channels. (Adapted, with permission, from Hodgkin and Huxley 1952.)

currents,  $I_K$  and  $I_l$ , by increasing the electrochemical driving forces acting on  $\text{K}^+$  and  $\text{Cl}^-$ . In addition, the depolarization augments  $g_K$  by gradually opening more voltage-gated  $\text{K}^+$  channels (Figure 7-7). As the outward  $I_K$  and  $I_l$  increase with depolarization they repolarize the membrane and resist the depolarizing action of the  $\text{Na}^+$  influx. However, because of the high voltage sensitivity and more rapid kinetics of activation of the  $\text{Na}^+$  channels, the depolarization eventually reaches a point where the increase in inward  $I_{\text{Na}}$  exceeds the increase in outward  $I_K$  and  $I_l$ . At this point there is a net inward ionic current. This produces a further depolarization, opening even more  $\text{Na}^+$  channels, so that the depolarization becomes regenerative, driving the membrane potential all the way to the peak of the action potential. The specific value of  $V_m$  at which the net ionic current ( $I_{\text{Na}} + I_K + I_l$ ) just changes from outward to inward, depositing a net positive charge on the inside of the membrane capacitance, is the threshold.

### Variations in the Properties of Voltage-Gated Ion Channels Expand the Signaling Capabilities of Neurons

The basic mechanism of electrical excitability identified by Hodgkin and Huxley in the squid giant axon appears to be universal in all excitable cells: Voltage-gated channels conduct an inward  $\text{Na}^+$  current followed by an

outward  $\text{K}^+$  current. However, we now know that there are many types of voltage-gated  $\text{Na}^+$  and  $\text{K}^+$  channels encoded by families of related genes that are expressed in different nerve and muscle cells.

The biophysical properties of the various  $\text{Na}^+$  and  $\text{K}^+$  channels can differ both quantitatively and qualitatively from the channels characterized by Hodgkin and Huxley. Other gene families encode voltage-gated channels that select for  $\text{Ca}^{2+}$  ions or have mixed permeability to  $\text{Na}^+$  and  $\text{K}^+$ . Moreover, the distribution of these channels can vary between different types of neurons, and can even vary as a function of locale within a single neuron. These differences in the pattern of ion channel expression have important consequences for membrane excitability, as we shall now explore.

### The Nervous System Expresses a Rich Variety of Voltage-Gated Ion Channels

Voltage-gated  $\text{Na}^+$  and  $\text{K}^+$  channels similar to those described by Hodgkin and Huxley have been found in almost every type of neuron examined. In addition, most neurons contain voltage-gated  $\text{Ca}^{2+}$  channels that open in response to membrane depolarization. A strong electrochemical gradient drives  $\text{Ca}^{2+}$  into the cell, so these channels give rise to an inward  $I_{\text{Ca}}$  that helps depolarize the cell.

Some neurons and muscle cells have voltage-gated  $\text{Cl}^-$  channels that contribute to membrane repolarization. Many neurons have cation channels that are slowly activated by hyperpolarization (instead of the usual depolarization). These hyperpolarization-activated cation (or HCN) channels are permeable to both  $\text{K}^+$  and  $\text{Na}^+$  and have a reversal potential around  $-40$  to  $-30$  mV. As a result, they give rise to an inward depolarizing current, referred to as  $I_h$ , when the membrane repolarizes to negative resting potentials or becomes hyperpolarized during synaptic inhibition.

Each basic type of ion channel has many variants. For example, several types of voltage-activated  $\text{K}^+$  channels differ in their kinetics of activation, voltage-activation range, and sensitivity to various ligands. Four of these variants are particularly important in the nervous system. (1) The slowly activating  $\text{K}^+$  channel described by Hodgkin and Huxley is called the *delayed rectifier*. (2) The *calcium-activated  $\text{K}^+$  channel* is activated by an increase in intracellular  $\text{Ca}^{2+}$  when nearby voltage-gated  $\text{Ca}^{2+}$  channels open in response to depolarization. One subclass of calcium-activated  $\text{K}^+$  channels is voltage-dependent. However, in the absence of  $\text{Ca}^{2+}$  the channel requires very large, nonphysiological depolarization to open. The binding of  $\text{Ca}^{2+}$  to a site on the cytoplasmic surface of the channel shifts its voltage-gating

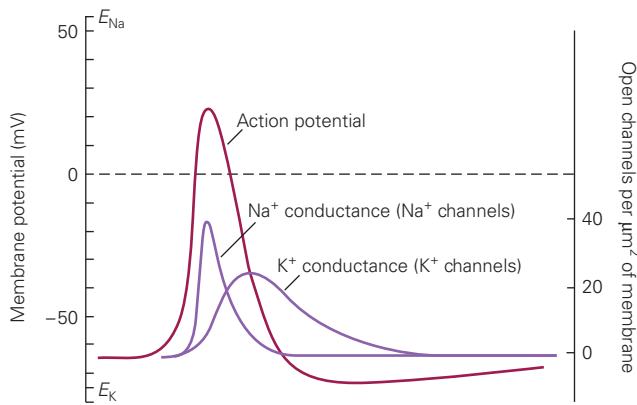


**Figure 7-10** The sequential opening of voltage-gated  $\text{Na}^+$  and  $\text{K}^+$  channels generates the action potential. One of Hodgkin and Huxley's great achievements was to dissect the change in conductance during an action potential into separate components attributable to the opening of  $\text{Na}^+$  and  $\text{K}^+$  channels. The shape of the action potential and the underlying conductance changes can be calculated from the properties of the voltage-gated  $\text{Na}^+$  and  $\text{K}^+$  channels. (Adapted, with permission, from Hodgkin and Huxley 1952.)

currents,  $I_K$  and  $I_l$ , by increasing the electrochemical driving forces acting on  $\text{K}^+$  and  $\text{Cl}^-$ . In addition, the depolarization augments  $g_K$  by gradually opening more voltage-gated  $\text{K}^+$  channels (Figure 7-7). As the outward  $I_K$  and  $I_l$  increase with depolarization they repolarize the membrane and resist the depolarizing action of the  $\text{Na}^+$  influx. However, because of the high voltage sensitivity and more rapid kinetics of activation of the  $\text{Na}^+$  channels, the depolarization eventually reaches a point where the increase in inward  $I_{\text{Na}}$  exceeds the increase in outward  $I_K$  and  $I_l$ . At this point there is a net inward ionic current. This produces a further depolarization, opening even more  $\text{Na}^+$  channels, so that the depolarization becomes regenerative, driving the membrane potential all the way to the peak of the action potential. The specific value of  $V_m$  at which the net ionic current ( $I_{\text{Na}} + I_K + I_l$ ) just changes from outward to inward, depositing a net positive charge on the inside of the membrane capacitance, is the threshold.

### Variations in the Properties of Voltage-Gated Ion Channels Expand the Signaling Capabilities of Neurons

The basic mechanism of electrical excitability identified by Hodgkin and Huxley in the squid giant axon appears to be universal in all excitable cells: Voltage-gated channels conduct an inward  $\text{Na}^+$  current followed by an

outward  $\text{K}^+$  current. However, we now know that there are many types of voltage-gated  $\text{Na}^+$  and  $\text{K}^+$  channels encoded by families of related genes that are expressed in different nerve and muscle cells.

The biophysical properties of the various  $\text{Na}^+$  and  $\text{K}^+$  channels can differ both quantitatively and qualitatively from the channels characterized by Hodgkin and Huxley. Other gene families encode voltage-gated channels that select for  $\text{Ca}^{2+}$  ions or have mixed permeability to  $\text{Na}^+$  and  $\text{K}^+$ . Moreover, the distribution of these channels can vary between different types of neurons, and can even vary as a function of locale within a single neuron. These differences in the pattern of ion channel expression have important consequences for membrane excitability, as we shall now explore.

### The Nervous System Expresses a Rich Variety of Voltage-Gated Ion Channels

Voltage-gated  $\text{Na}^+$  and  $\text{K}^+$  channels similar to those described by Hodgkin and Huxley have been found in almost every type of neuron examined. In addition, most neurons contain voltage-gated  $\text{Ca}^{2+}$  channels that open in response to membrane depolarization. A strong electrochemical gradient drives  $\text{Ca}^{2+}$  into the cell, so these channels give rise to an inward  $I_{\text{Ca}}$  that helps depolarize the cell.

Some neurons and muscle cells have voltage-gated  $\text{Cl}^-$  channels that contribute to membrane repolarization. Many neurons have cation channels that are slowly activated by hyperpolarization (instead of the usual depolarization). These hyperpolarization-activated cation (or HCN) channels are permeable to both  $\text{K}^+$  and  $\text{Na}^+$  and have a reversal potential around  $-40$  to  $-30$  mV. As a result, they give rise to an inward depolarizing current, referred to as  $I_h$ , when the membrane repolarizes to negative resting potentials or becomes hyperpolarized during synaptic inhibition.

Each basic type of ion channel has many variants. For example, several types of voltage-activated  $\text{K}^+$  channels differ in their kinetics of activation, voltage-activation range, and sensitivity to various ligands. Four of these variants are particularly important in the nervous system. (1) The slowly activating  $\text{K}^+$  channel described by Hodgkin and Huxley is called the *delayed rectifier*. (2) The *calcium-activated  $\text{K}^+$  channel* is activated by an increase in intracellular  $\text{Ca}^{2+}$  when nearby voltage-gated  $\text{Ca}^{2+}$  channels open in response to depolarization. One subclass of calcium-activated  $\text{K}^+$  channels is voltage-dependent. However, in the absence of  $\text{Ca}^{2+}$  the channel requires very large, nonphysiological depolarization to open. The binding of  $\text{Ca}^{2+}$  to a site on the cytoplasmic surface of the channel shifts its voltage-gating



to allow the channel to open at more negative potentials. (3) The *A-type K<sup>+</sup> channel* is activated rapidly by depolarization, almost as rapidly as the Na<sup>+</sup> channel; like the Na<sup>+</sup> channel, it also inactivates rapidly if the depolarization is prolonged. (4) The *M-type K<sup>+</sup> channel* requires only small depolarizations from the resting potential to open; however, it activates very slowly, requiring tens of milliseconds to open. One distinctive feature of the M-type channel is that it is *closed* by a neurotransmitter, acetylcholine.

Similarly, at least five major types of voltage-gated Ca<sup>2+</sup> channels and eight types of voltage-gated Na<sup>+</sup> channels are expressed in the nervous system. Each of these major subtypes is encoded by a different gene and has several structural and functional variants that are generated through alternative splicing or by combining the pore-forming  $\alpha$ -subunit with different types of auxiliary subunits.

The squid axon can generate an action potential with just two types of voltage-gated channels. Why then are so many types of voltage-gated ion channels found in the nervous system? The answer is that neurons with a greater variety of voltage-gated channels have much more complex information-processing abilities than those with only two types of channels. Some ways in which various voltage-gated channels influence neuronal function are described below.

### Gating of Voltage-Sensitive Ion Channels Can Be Influenced by Various Cytoplasmic Factors

In a typical neuron the opening and closing of certain voltage-gated ion channels can be modulated by various cytoplasmic factors, thus affording the neuron's excitability properties greater flexibility. Changes in the levels of such cytoplasmic factors may result from the activity of the neuron itself or from the influences of other neurons.

Calcium concentration is one important cytoplasmic factor that modulates ion channel activity. The ionic current through membrane channels during an action potential generally does not result in appreciable changes in the intracellular concentrations of most ion species. Calcium is a notable exception to this rule. The concentration of free Ca<sup>2+</sup> in the cytoplasm of a resting cell is extremely low, about 10<sup>-7</sup> M, several orders of magnitude below the external Ca<sup>2+</sup> concentration, which is approximately 2 mM. For this reason the intracellular Ca<sup>2+</sup> concentration may increase many fold above its resting value as a result of the influx of Ca<sup>2+</sup> through voltage-gated Ca<sup>2+</sup> channels. The transient increase in Ca<sup>2+</sup> concentration near the inside of the membrane enhances the probability that calcium-activated,

voltage-sensitive K<sup>+</sup> channels will open. Some Ca<sup>2+</sup> channels are themselves sensitive to levels of intracellular Ca<sup>2+</sup>, becoming inactivated when incoming Ca<sup>2+</sup> binds to their intracellular surface. Changes in the intracellular concentration of Ca<sup>2+</sup> can also influence a variety of cellular metabolic processes, including neurotransmitter release and gene expression.

The activity of voltage-gated channels can also be regulated by the action of neurotransmitters through the recruitment of second-messenger pathways (see Chapter 11). These pathways can alter channel activity through a number of mechanisms, including direct phosphorylation of the intracellular domains of a channel or direct binding of cyclic nucleotides or membrane phosphoinositides to specialized binding domains in certain types of channels. As is true for the effects of Ca<sup>2+</sup> binding, these pathways typically affect the kinetics or voltage sensitivity of channel gating rather than ion permeability of the open channel. The importance of cytoplasmic Ca<sup>2+</sup> and other second messengers in the control of neuronal activity will become evident in many contexts throughout this book.

### Excitability Properties Vary Between Regions of the Neuron

Different regions of a neuron have different types of ion channels that support the specialized functions of each region. The axon, for example, specializes in carrying signals faithfully over long distances; as such it functions as a relatively simple relay line. In contrast, the input, integrative, and output regions of a neuron (see Figure 2–9) typically perform more complex processing of the information they receive before passing it along.

Dendrites in many types of neurons have voltage-gated ion channels, including Ca<sup>2+</sup>, K<sup>+</sup>, HCN, and Na<sup>+</sup> channels. When activated, these channels help shape the amplitude, time course, and propagation of the synaptic potentials to the cell body. In some neurons action potentials may be propagated from the trigger zone at the initial segment of the axon back into the dendrites, thereby influencing synaptic integration in the dendrites. In other neurons the density of voltage-gated channels in the dendrites is sufficient to support the generation of a local action potential, which may then be conducted through the cell soma to the axon initial segment.

The trigger zone at the axon initial segment has the lowest threshold for action potential generation in part because it has an exceptionally high density of voltage-gated Na<sup>+</sup> channels. In addition, it typically has voltage-gated ion channels that are sensitive to relatively small deviations from the resting potential.



These channels thus play a critical role in the transformation of graded synaptic or receptor potentials into a train of all-or-none action potentials. Examples include the M-type and certain A-type  $K^+$  channels, and a class of low voltage-activated  $Ca^{2+}$  channels (see below).

Conduction of the action potential down the axon is mediated primarily by voltage-gated  $Na^+$  and  $K^+$  channels that function much like those in the squid axon. In peripheral myelinated axons the mechanism of action potential repolarization at the nodes of Ranvier is particularly simple—the spike is terminated by fast inactivation of  $Na^+$  channels combined with a large outward  $K^+$  leakage current. Voltage-gated  $K^+$  channels play a relatively minor role in action potential repolarization in these peripheral axons. In contrast, some central myelinated axons have significant numbers of voltage-gated  $K^+$  channels at their nodes important for repolarization. Moreover, both central and peripheral myelinated axons have fairly high densities of  $K^+$  channels under the myelin sheath near the two ends of each internodal segment. The normal function of these  $K^+$  channels is to suppress any action potential that may be generated by axon membrane under the myelin sheath. In demyelinating diseases these channels become exposed and thus inhibit the ability of the bare axon to conduct action potentials (see Chapter 6).

Presynaptic nerve terminals at chemical synapses commonly have a high density of voltage-gated  $Ca^{2+}$  channels. Arrival of an action potential in the terminal opens these channels, causing an influx of  $Ca^{2+}$  that triggers transmitter release (Chapter 12).

### Excitability Properties Vary Between Types of Neurons

Through the expression of a distinct complement of ion channels, the electrical properties of a neuron can be fine-tuned to match the dynamic demands of the information that it processes. Thus, although the function of a neuron is defined to a great extent by its synaptic inputs and outputs to other neurons, the excitability properties of the cell are also a critical factor in cell function.

Two aspects of excitability are important: (1) control of the shape of the action potential and (2) spike encoding, the process by which receptor potentials or synaptic potentials are converted into a temporal pattern of action potentials. Both of these features vary widely between different types of neurons. Of the voltage-gated channels, the  $K^+$  channels exhibit the greatest functional diversity. Differences in  $K^+$  channel expression are a key factor in determining the distinctive excitability properties of different classes of neurons.

How a neuron responds to synaptic input is determined by the proportions of different types of voltage-gated channels in the cell's input and integrative regions. For example, cells with different combinations of channels respond differently to a constant excitatory input. Some cells respond with only a single action potential, others with a train of action potentials at a constant rate of firing, and still others with either an accelerating or decelerating train of action potentials. The combined presence of certain voltage-gated  $Ca^{2+}$  channels and HCN channels generates pacemaker currents that allow some neurons to fire spontaneously in the absence of any external input (Figure 7–11D).

The firing rate of most neurons saturates as the strength of synaptic input increases, with a maximal rate that is not particularly high. However, certain classes of neurons have an unusually wide dynamic range and are able to fire at very high frequencies because of an unusually brief refractory period. This high firing rate is of particular importance in the auditory system, where neurons must respond to sound waves of very high frequencies. The short refractory period is caused, in part, by the expression in the auditory neurons of the voltage-gated  $K^+$  channel Kv3, whose activation gates close extremely rapidly following repolarization, resulting in a very short hyperpolarizing after-potential.

Some types of synaptic inputs to a neuron modulate the function of voltage-gated channels and thereby modulate the cell's response to other inputs. For example, in some neurons a steady hyperpolarizing synaptic input makes the cell less excitable by reducing the extent of inactivation of the A-type  $K^+$  channels that occurs at the normal resting potential of the cell. In other neurons such a steady hyperpolarization makes the cell *more* excitable because it reduces the inactivation of a particular class of voltage-gated  $Ca^{2+}$  channels. The firing properties of neurons can also be modulated by changing the function of certain voltage-gated ion channels, such as the M-type  $K^+$  channels, through synaptic activation of second messengers (Figure 7–11A–C).

Although the action potentials in a neuron under constant conditions are constant in shape, action potential duration and amplitude can vary depending on intrinsic neuronal activity and extrinsic synaptic inputs. Such changes can be particularly prominent in the input and output regions of the neuron. The longer the duration of the action potential, the longer the voltage-gated ion channels stay open and thus the greater the  $Ca^{2+}$  influx through voltage-gated  $Ca^{2+}$  channels. Changes in duration of the action potential therefore can play an important role in influencing events that are sensitive to cytoplasmic  $Ca^{2+}$  levels, such as ion channel

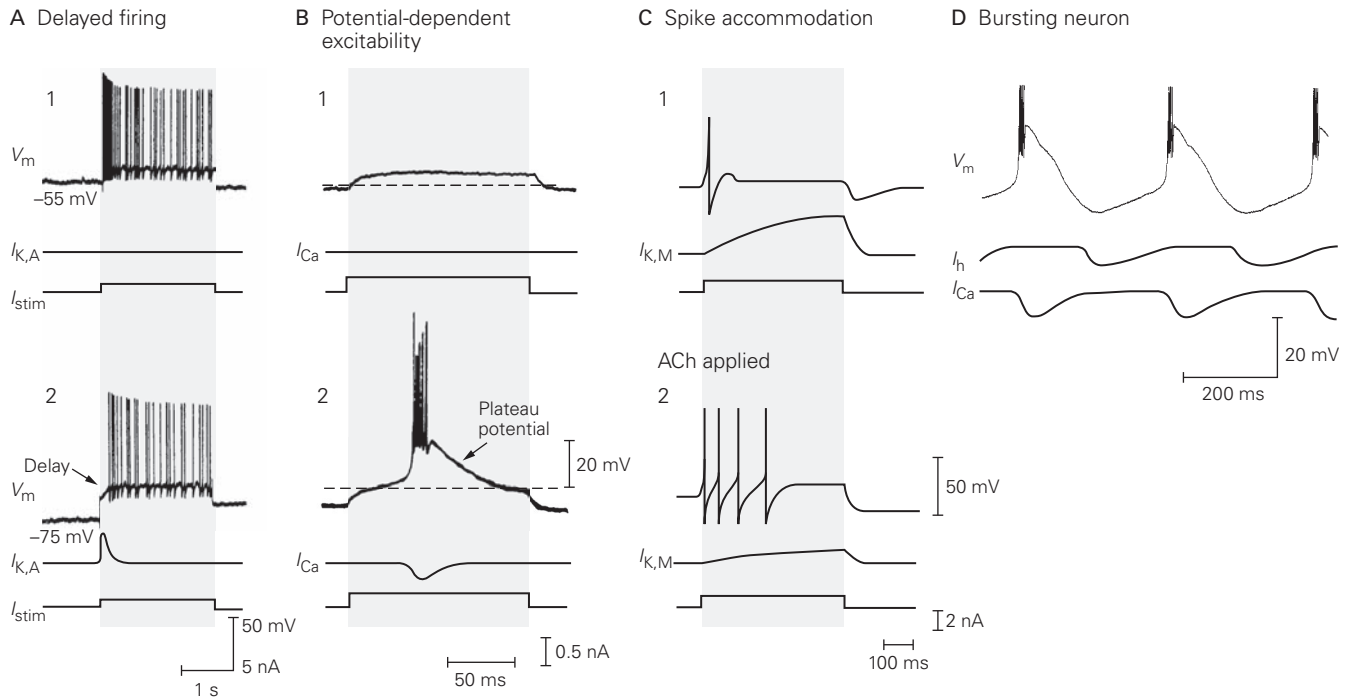


**Figure 7-11** The response of a neuron to synaptic input is determined by its complement of voltage-gated ion channels. The waveform of the ionic current traces in the figure is drawn to reflect the activation and inactivation of the underlying conductances during the slow subthreshold changes in membrane potential. In reality, the currents will also show rapid changes during any triggered action potentials because of large, rapid changes in driving force.

**A.** Injection of a depolarizing current pulse ( $I_{stim}$ ) into a neuron in the nucleus tractus solitarius normally triggers an immediate train of action potentials (1). If the cell is first held at a hyperpolarized membrane potential, the spike train is delayed (2). The delay is caused by A-type  $K^+$  channels, which are activated by depolarizing synaptic input. The opening of these channels generates a transient outward  $K^+$  current,  $I_{K,A}$ , that briefly drives  $V_m$  away from threshold. These channels typically are inactivated at the resting potential ( $-55$  mV), but steady hyperpolarization removes the inactivation. (Reproduced, with permission, from Dekin and Getting 1987.)

**B.** A small depolarizing current pulse injected into a thalamic neuron at rest generates a subthreshold depolarization (1). If the membrane potential is held at a hyperpolarized level, the same current pulse triggers a burst of action potentials (2). The effectiveness of the current pulse is enhanced because the hyperpolarization causes a type of voltage-gated  $Ca^{2+}$  channel to recover from inactivation. Depolarizing inward current through the  $Ca^{2+}$  channels ( $I_{Ca}$ ) generates a plateau potential of about 20 mV that triggers a burst of action potentials. The dashed line indicates the level of the normal resting potential. (Reproduced, with permission, from Llinás and Jahnsen 1982.)

The data in parts A and B demonstrate that steady hyperpolarization, such as might be produced by inhibitory synaptic input to a neuron, can profoundly affect the spike train pattern of a neuron. This effect varies greatly among cell types and

depends on the presence or absence of particular types of voltage-gated  $Ca^{2+}$  and  $K^+$  channels.

**C.** The firing properties of sympathetic neurons in autonomic ganglia are regulated by a neurotransmitter. (1) A prolonged depolarizing current normally results in a single action potential. The depolarization turns on a slowly activated  $K^+$  current, the M current ( $I_{K,M}$ ). The slow activation kinetics of the M-type channels allow the cell to fire one action potential before the efflux of  $K^+$  through the M-type channels becomes sufficient to shift the membrane to more negative voltages and prevent the cell from firing more action potentials (a process termed *accommodation*). (2) Synaptic release of the neurotransmitter acetylcholine (ACh) onto this neuron activates a second-messenger pathway that closes the M-type channels, allowing the cell to fire many action potentials in response to the same stimulus. (See also Figure 11-11.) (Reproduced, with permission, from Jones and Adams 1987.)

**D.** In the absence of synaptic input, thalamocortical relay neurons can fire spontaneously in brief bursts of action potentials. These bursts are produced by current through two types of voltage-gated ion channels. The gradual depolarization that leads to a burst is driven by inward current through HCN channels ( $I_h$ ), which have the unusual property of opening in response to hyperpolarizing voltage steps. The firing burst is triggered by an inward  $Ca^{2+}$  current through voltage-gated  $Ca^{2+}$  channels that are activated at relatively low levels of depolarization. This  $Ca^{2+}$  influx generates sufficient depolarization to reach threshold and drive a brief burst of  $Na^+$ -dependent action potentials. The strong depolarization during the burst causes the HCN channels to close and inactivates the  $Ca^{2+}$  channels, allowing hyperpolarization to develop between bursts of firing. This hyperpolarization then opens the HCN channels, initiating the next cycle in the rhythm. (Reproduced, with permission, from McCormick and Huguenard 1992.)

gating, transmitter release, long-term changes in synaptic strength, and gene expression.

Extrinsic synaptic inputs can modulate action potential shape by activating second-messenger pathways that modulate the activity of certain voltage-gated ion channels (see Chapter 11). The most common intrinsic modulation occurs during high-frequency firing, when there is a progressive buildup of inactivation of voltage-gated  $K^+$  channels that leads to a progressive increase in the duration of the later action potentials in a train. Some of the functional implications of these changes in action potential shape are considered in later chapters.

### The Mechanisms of Voltage-Gating and Ion Permeation Have Been Inferred from Electrophysiological Measurements

The empirical equations derived by Hodgkin and Huxley are quite successful in describing how the flow of ions through the  $Na^+$  and  $K^+$  channels generates the action potential. However, these equations describe the process of excitation primarily in terms of changes in membrane conductance and current. They tell little about the mechanisms that activate or inactivate channels in response to changes in membrane potential or selectivity for specific ions.

Our understanding of the properties of ion channel molecules was greatly enhanced by patch-clamp studies of current through single channels (see Box 5-1). Patch-clamp experiments demonstrate that voltage-gated channels generally have only two conductance states, open and closed. Recordings of single voltage-gated  $Na^+$  channels show that, in response to a depolarization, a channel opens in an all-or-none fashion, conducting brief current pulses of constant amplitude but variable duration (Figure 7-12). During a maintained depolarization the open state of a channel is rapidly terminated by inactivation. Typical conductances of single voltage-gated  $Na^+$ ,  $K^+$ , and  $Ca^{2+}$  channels range from 1 to 20 pS, depending on channel type. One class of calcium-activated  $K^+$  channel has an unusually large conductance of approximately 200 pS.

#### Voltage-Gated Sodium Channels Open and Close in Response to Redistribution of Charges Within the Channel

In their original study of the squid axon, Hodgkin and Huxley suggested that a voltage-gated channel has a net charge, the *gating charge*, somewhere within the membrane. They postulated that a change in membrane

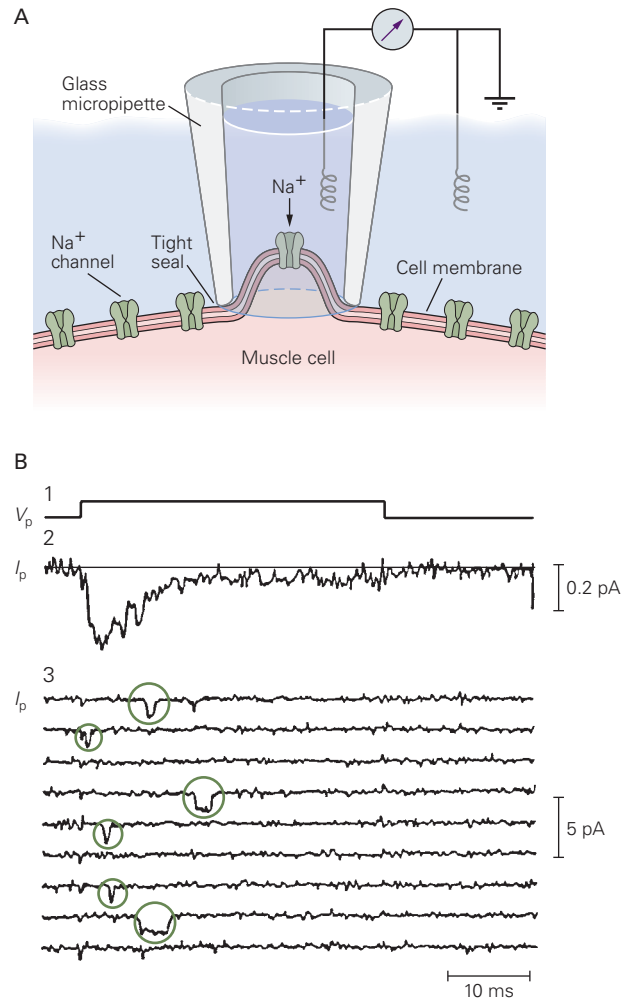


**Figure 7-12** Individual voltage-gated channels open in an all-or-none fashion.

**A.** A small patch of membrane containing a single voltage-gated  $Na^+$  channel is electrically isolated from the rest of the cell by the patch electrode. The  $Na^+$  current that enters the cell through the channel is recorded by a current monitor connected to the patch electrode (see Box 5-1).

**B.** Recordings of single  $Na^+$  channels in cultured muscle cells of rats. (1) Time course of a 10 mV depolarizing voltage step applied across the isolated patch of membrane ( $V_p$  = potential difference across the patch). (2) The sum of the inward current through the  $Na^+$  channel in the patch during 300 trials ( $I_p$  = current through the patch). The trace was obtained by blocking the  $K^+$  channels with tetraethylammonium and subtracting the leakage and capacitive currents electronically. (3) Nine individual trials from the set of 300, showing six openings of the channel (circles). These data demonstrate that the total  $Na^+$  current recorded in a conventional voltage-clamp record (see Figure 7-3B) can be accounted for by the all-or-none opening and closing of a large number of  $Na^+$  channels. (Reproduced, with permission, from Sigworth and Neher 1980.)

potential causes this charge to move across the electric field of the membrane, resulting in conformational changes that open or close the channel.

They further predicted that the movement of charge would be measurable. For example, they postulated that depolarization would move a positive gating charge from near the inner surface toward the outer surface of the membrane, owing to the interaction of the charge with the membrane electric field. This displacement would reduce the net separation of charge across the membrane and hence tend to hyperpolarize the membrane. To keep the membrane potential constant in a voltage-clamp experiment, a small extra component of outward capacitive current, called *gating current*, would have to be generated by the voltage clamp to counteract this rearrangement of charge within the membrane.

These predictions of Hodgkin and Huxley were later confirmed when the membrane current was examined by means of very sensitive techniques. The

gating current was found to flow at the beginning and end of a depolarizing voltage-clamp step prior to the opening or closing of the  $\text{Na}^+$  channels (Figure 7-13).

Analysis of the gating current has provided additional insights into the mechanisms of voltage-gating. For example, it has revealed that activation and inactivation of  $\text{Na}^+$  channels are coupled processes. During a short depolarizing pulse the net outward movement of gating charge within the membrane at the beginning of the pulse is balanced by an equal and opposite movement of gating charge at the end of the pulse. However, if the pulse lasts long enough for  $\text{Na}^+$  channel inactivation to take place, the movement of gating charge back across the membrane at the end of the pulse is delayed. Some of the gating charge is thus temporarily immobilized; only as the  $\text{Na}^+$  channels recover from inactivation is that charge free to move back across the membrane. This charge immobilization indicates that some of the gating charges cannot move while the inactivation gate is closed.

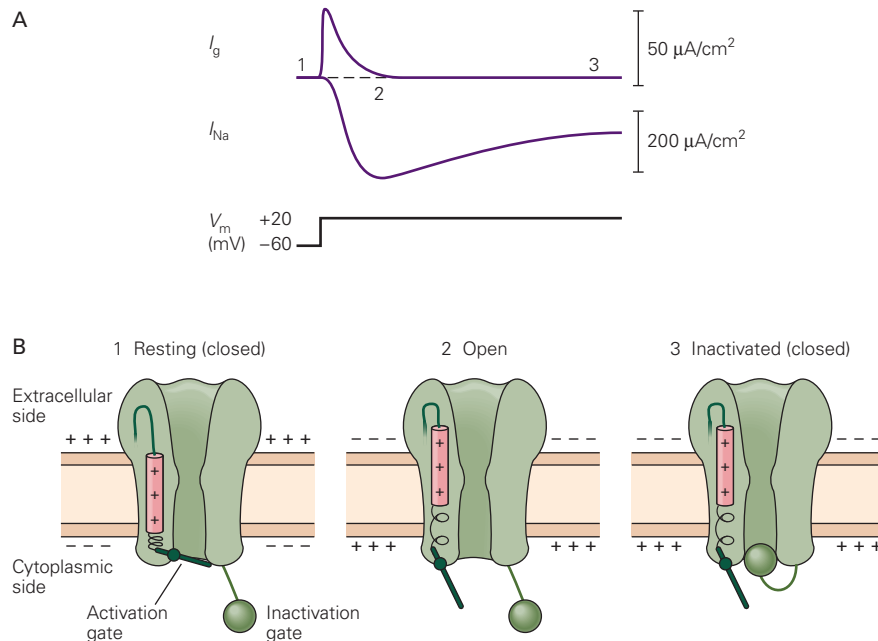


**Figure 7-13** Changes in charge distribution within the  $\text{Na}^+$  channel are associated with opening and closing of the channel.

**A.** When the membrane is depolarized, the  $\text{Na}^+$  current ( $I_{\text{Na}}$ ) is activated and then inactivated. The activation of the  $\text{Na}^+$  current is preceded by a brief outward current ( $I_g$ ), reflecting the outward movement of positive charges within the  $\text{Na}^+$  channels associated with the opening of their activation gates. To detect this small gating current it is necessary to block the flow of ionic current through the  $\text{Na}^+$  and  $\text{K}^+$  channels and mathematically subtract the

capacitive current due to charging of the lipid bilayer. (Adapted, with permission, from Armstrong and Gilly 1979).

**B.** The redistribution of gating charge and positions of the activation and inactivation gates when the channel is at rest, open, and inactivated. The red cylinder represents a positively charged region containing the gating charge that is thought to move through the membrane electric field in response to voltage changes. Depolarization from the resting state causes the gating charge to move outward, opening the activation gate. Inactivation closes the channel, immobilizing the gating charge.

To explain this immobilization phenomenon, Clay Armstrong and Francisco Bezanilla proposed that  $\text{Na}^+$  channel inactivation occurs when the open (activated) channel is blocked by a tethered plug (a ball and chain mechanism), thereby preventing the closure of the activation gate (Figure 7–13B). In support of this idea, exposing the inside of the axon to proteolytic enzymes selectively eliminates inactivation and its effect on gating charge. The  $\text{Na}^+$  channels remain open during a depolarization, and gating charge immobilization at the end of the pulse is eliminated—presumably because the enzymes clip off the inactivation “ball.”

### Voltage-Gated Sodium Channels Select for Sodium on the Basis of Size, Charge, and Energy of Hydration of the Ion

In Chapter 5 we saw how the structure of the  $\text{K}^+$  channel pore could explain how such channels are able to select for  $\text{K}^+$  over  $\text{Na}^+$  ions. The narrow diameter of the  $\text{K}^+$  channel selectivity filter (around 0.3 nm) requires that a  $\text{K}^+$  or  $\text{Na}^+$  ion must shed nearly all of its waters of hydration to enter the channel, an energetically unfavorable event.

The energetic cost of dehydration of a  $\text{K}^+$  ion is well compensated by its close interaction with a cage of electronegative carbonyl oxygen atoms contributed by the peptide backbones of the four subunits of the  $\text{K}^+$  channel selectivity filter. Because of its smaller radius, a  $\text{Na}^+$  ion has a higher local electric field than does a  $\text{K}^+$  ion and therefore interacts more strongly with its waters of hydration than does  $\text{K}^+$ . On the other hand, the small diameter of the  $\text{Na}^+$  ion precludes close interaction with the cage of carbonyl oxygen atoms in the selectivity filter; the resultant high energetic cost of dehydrating the  $\text{Na}^+$  ion excludes it from entering the channel.

How then does the selectivity filter of the  $\text{Na}^+$  channel select for  $\text{Na}^+$  over  $\text{K}^+$  ions? Bertil Hille was able to deduce a model for the  $\text{Na}^+$  channel’s selectivity mechanism from measurements of the channel’s relative permeability to several types of organic and inorganic cations that differ in size and hydrogen-bonding characteristics. As we learned in Chapter 5, the channel behaves as if it contains a filter or recognition site that selects partly on the basis of size, thus acting as a molecular sieve (see Figure 5–1). Based on the size of the largest organic cation that could readily permeate the channel, Hille deduced that the selectivity filter had rectangular dimensions of  $0.3 \times 0.5$  nm. This cross section is just large enough to accommodate one  $\text{Na}^+$  ion contacting one water molecule. Cations that are larger in diameter cannot pass through the pore. Cations smaller than this critical size pass through the pore, but only after losing most of the waters of hydration they normally carry in free solution.

The ease with which organic cations with good hydrogen-bonding characteristics pass through the channel suggests that part of the inner wall of the channel is made up of negatively polarized or charged amino acid residues that can substitute for the ion’s waters of hydration. Lowering the pH of the fluid surrounding the cell reduces the conductance of the open channel, consistent with the titration of an important negatively charged carboxylic acid residue.

Based on these findings, Hille proposed that  $\text{Na}^+$  channels select for ions by the following mechanism. Negatively charged carboxylic acid groups of glutamate or aspartate residues at the outer mouth of the pore perform the first step in the selection process by attracting cations and repelling anions. The negative carboxylic acid groups, as well as other oxygen atoms that line the pore, can substitute for waters of hydration, but the degree of effectiveness of this substitution varies among ion species. For example, the negative charge of a carboxylic acid is able to form a stronger coulombic interaction with the smaller  $\text{Na}^+$  ion compared to the larger  $\text{K}^+$  ion. Because the  $\text{Na}^+$  channel is large enough to accommodate a cation in contact with several water molecules, the energetic cost of dehydration is not as great as it is in a  $\text{K}^+$  channel. As a result of these two features, the  $\text{Na}^+$  channel is able to select for  $\text{Na}^+$  over  $\text{K}^+$ . A recent X-ray crystal structure of a bacterial voltage-gated  $\text{Na}^+$  channel has confirmed many of the key features of Hille’s model.

### Voltage-Gated Potassium, Sodium, and Calcium Channels Stem from a Common Ancestor and Have Similar Structures

Detailed molecular studies have revealed that all voltage-gated cation channels—those permeant to  $\text{K}^+$ ,  $\text{Na}^+$ , or  $\text{Ca}^{2+}$ —have a similar underlying architecture. In fact, there is now strong evidence from studies of bacteria, plants, invertebrates, and vertebrates that most voltage-sensitive cation channels stem from a common ancestral channel—perhaps a  $\text{K}^+$  channel—that can be traced to a single-cell organism living more than 1.4 billion years ago, before the evolution of separate plant and animal kingdoms. The amino acid sequences that are highly conserved through evolution help identify the domains within contemporary voltage-gated cation channels that are critical for function.

Voltage-gated cation channels are composed of pore-forming  $\alpha$ -subunits that each contain a motif consisting of six transmembrane segments (S1–S6). A seventh hydrophobic region, the “P-region,” connects the S5 and S6 segments. It forms a loop that dips into and out of the extracellular side of the membrane and forms



the channel's selectivity filter. All voltage-gated  $K^+$  channels consist of four pore-forming subunits, each of which contributes one P-region to the pore of the fully assembled channel. Voltage-gated  $Na^+$  and  $Ca^{2+}$  channels consist of one large pore-forming subunit

containing four internal repeats of this basic motif (Figure 7–14). The amino acid sequence of the S5-P-S6 region of voltage-gated  $K^+$  channels is homologous to that of bacterial  $K^+$  channels with two transmembrane segments.

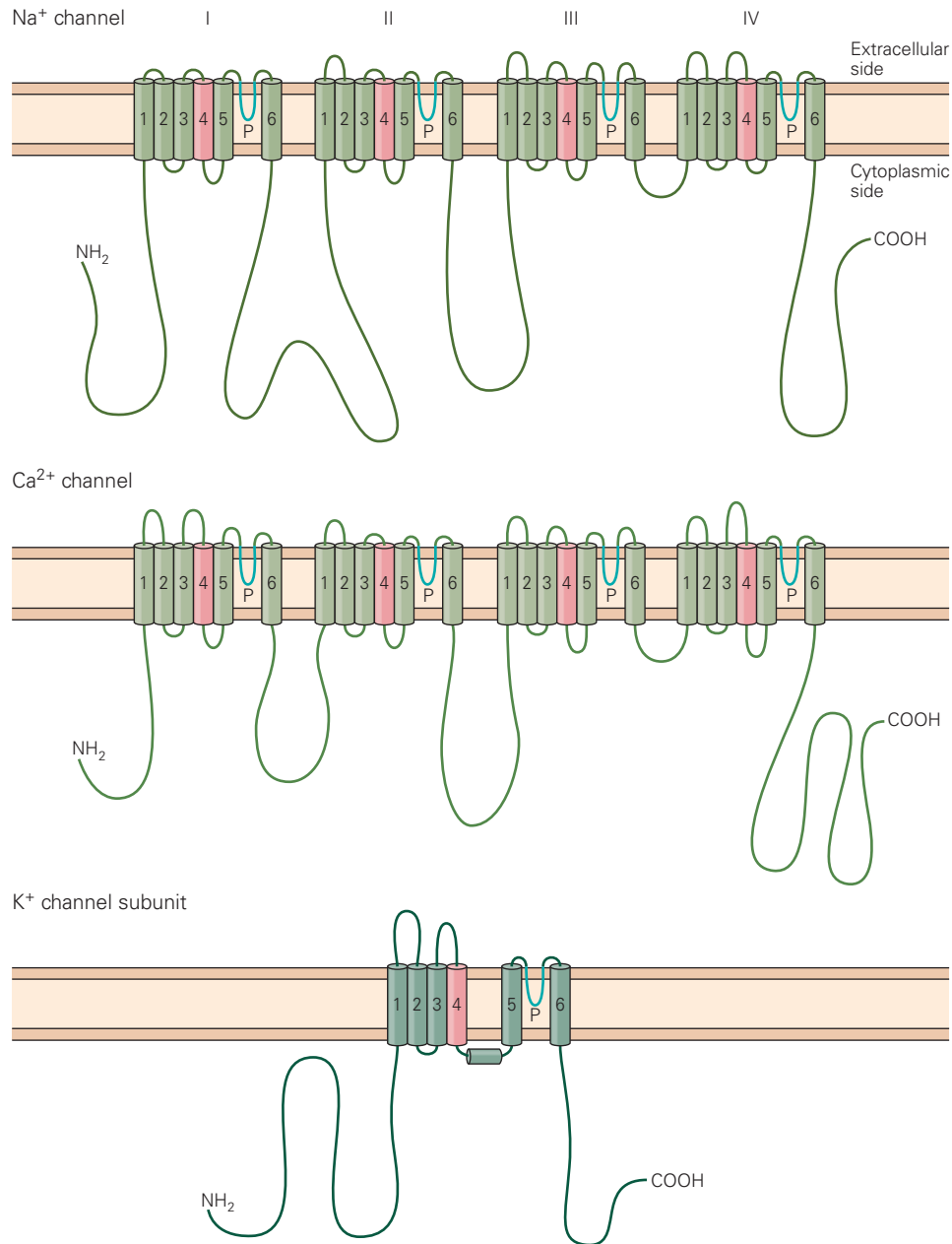


**Figure 7–14** The voltage-gated cation channels have homologous  $\alpha$ -subunit domains. The  $\alpha$ -subunit of the  $Na^+$  and  $Ca^{2+}$  channels consists of a single polypeptide chain with four homologous repeats (I–IV) of a basic motif that contains six membrane-spanning  $\alpha$ -helices (S1–S6). The P-region between  $\alpha$ -helices 5 and 6 that dips into and out of the

membrane forms the selectivity filter. The S4 segment has a net positive charge. The  $\alpha$ -subunit of the  $K^+$  channel, in contrast, has only one domain with six  $\alpha$ -helices and a P-region; four  $K^+$  channel  $\alpha$ -subunits are assembled to form a complete channel (see Figure 5–12A). (Adapted, with permission, from Catterall 1988; Stevens 1991.)

The S4 segment is thought to play a particularly important role in voltage-gating. This transmembrane segment contains a distinctive pattern of amino acids in which every third position contains a positively charged arginine or lysine residue. The presence of so many positive charges within a single transmembrane segment is highly unusual. Because this pattern of positive charges is present in all voltage-gated channels but is absent in channels that are not voltage-gated, it is thought that this region might be the voltage sensor—that part of the protein that transduces depolarization of the cell membrane into a conformational change that opens the channel. This idea is supported by experiments using site-directed mutagenesis, which show that neutralization of positive charges in S4 decreases the gating current and voltage sensitivity of channel activation.

### **X-Ray Crystallographic Analysis of Voltage-Gated Channel Structures Provides Insight into Voltage-Gating**

How do the positive charges in S4 move through the membrane electric field during channel gating? How is S4 movement coupled to gating? What is the relationship of the voltage-sensing region to the pore-forming region of the channel? Insights into such questions have been provided by recent X-ray crystallographic structures of mammalian delayed rectifier voltage-gated  $K^+$  channels performed by Rod MacKinnon and his colleagues, as well as by a number of studies using mutagenesis and other biophysical approaches.

The X-ray crystal structures of the Kv1.2 channel and a Kv1.2-2.1 chimera show that a  $K^+$  channel subunit is composed of two domains. The S1–S4 segments form a voltage-sensing domain at the periphery of the channel while the S5–P–S6 region forms the pore domain at the central axis of the channel (Figure 7–15). The idea that the S1–S4 voltage sensor is a separate domain is consistent with the recent finding that certain bacterial proteins contain S1–S4 domains but lack a pore domain. One such protein is a voltage-sensitive phosphatase and a second protein forms a voltage-gated proton channel.

In the two-transmembrane segment bacterial  $K^+$  channels the four inner transmembrane helices, which correspond to the S6 helices in voltage-gated  $K^+$  channels, form a tight bundle crossing at their cytoplasmic ends to form the gate of the channel (see Figure 5–16). In the open state the inner ends of these helices were seen to splay out to open the gate by bending at flexible glycine hinges. The structure of the Kv1.2-2.1 chimera indicates that the S6 helix is also bent at this conserved

glycine hinge so that the channel adopts an open conformation. It is not surprising that the Kv channel is in the open state as there is no voltage gradient across the channel in the crystals. This is similar to the situation in a membrane that has been depolarized to 0 mV, a voltage at which the channels are normally open.

One long-standing question in studies of voltage-gating is how the charges on the voltage-sensor overcome the unfavorable energy change associated with their positioning within the nonpolar membrane where they must sense the electric field. The crystal structure provides some answers to this question. Mutagenesis studies indicate that four positively charged arginine residues in the external half of the S4 segment are likely to carry most of the gating charge. In the open state the four positive charges face outward toward the extracellular side of the membrane, where they may undergo energetically favorable interactions with water or the negatively charged head groups of the phospholipid bilayer. Positive charges on other S4 residues that lie more deeply within the lipid bilayer are stabilized by interactions with negatively charged acidic residues on the S1–S3 transmembrane helices.

At present a crystal structure for the closed state of the channel is lacking. However, MacKinnon and colleagues have proposed a plausible model for voltage-gating based on the structures of the open voltage-gated  $K^+$  channel and the closed two-transmembrane segment bacterial  $K^+$  channel (Figure 7–16). According to this model, a negative voltage inside the cell exerts a force on the positively charged S4 helix that causes it to move inward by about 1.0 to 1.5 nm. As a result, the four positively charged S4 residues that in the depolarized state face the external environment and sense the extracellular potential now face the intracellular side of the membrane and sense the intracellular potential. In this manner movement of each S4 segment will translocate 3–4 electronic charges across the membrane electric field as the channel transitions between the closed and open states, for a total of 12–16 charges moved per tetrameric channel. This number is very similar to the total charge movement determined from gating current measurements.

How are S4 movements coupled to the gate of the channel? According to the model, the inward movement of the S4 segment when the membrane voltage becomes negative exerts a downward force on an  $\alpha$ -helix that couples the S4 and S5 transmembrane segments. This S4–S5 coupling helix lies roughly parallel to the membrane at its cytoplasmic surface. In the open state the S4–S5 helix rests on the inner end of the S6 helix gate. As a result, downward movement of the helix applies force to S6, closing the gate. Thus

voltage-gating is thought to rely on the electromechanical coupling between the voltage-sensing domain and the pore domain of the channel. Although this electro-mechanical coupling model provides a very satisfying picture for how changes in membrane voltage lead to channel gating, a definitive answer to this key problem will require resolution of the structure of the closed state of a voltage-gated channel.

### The Diversity of Voltage-Gated Channel Types Is Generated by Several Genetic Mechanisms

The conservative mechanism by which evolution proceeds—creating new structural or functional entities by duplicating, modifying, shuffling, and recombining existing gene-coding sequences—is illustrated by the modular design of the members of the extended gene family that encodes the voltage-gated  $\text{Na}^+$ ,  $\text{K}^+$ , and  $\text{Ca}^{2+}$  channels. This family also includes genes that encode calcium-activated  $\text{K}^+$  channels, the hyperpolarization-activated HCN channels, and a voltage-independent cyclic nucleotide-gated cation channel important for phototransduction and olfaction.

The functional differences between these channels are caused by differences in amino acid sequence in their core transmembrane domains as well as by the addition of regulatory domains to the C-terminal cytoplasmic end of the proteins. Some of these cytoplasmic domains bind either  $\text{Ca}^{2+}$  or cyclic nucleotides, enabling these agents to regulate channel gating (Figure 7–17).

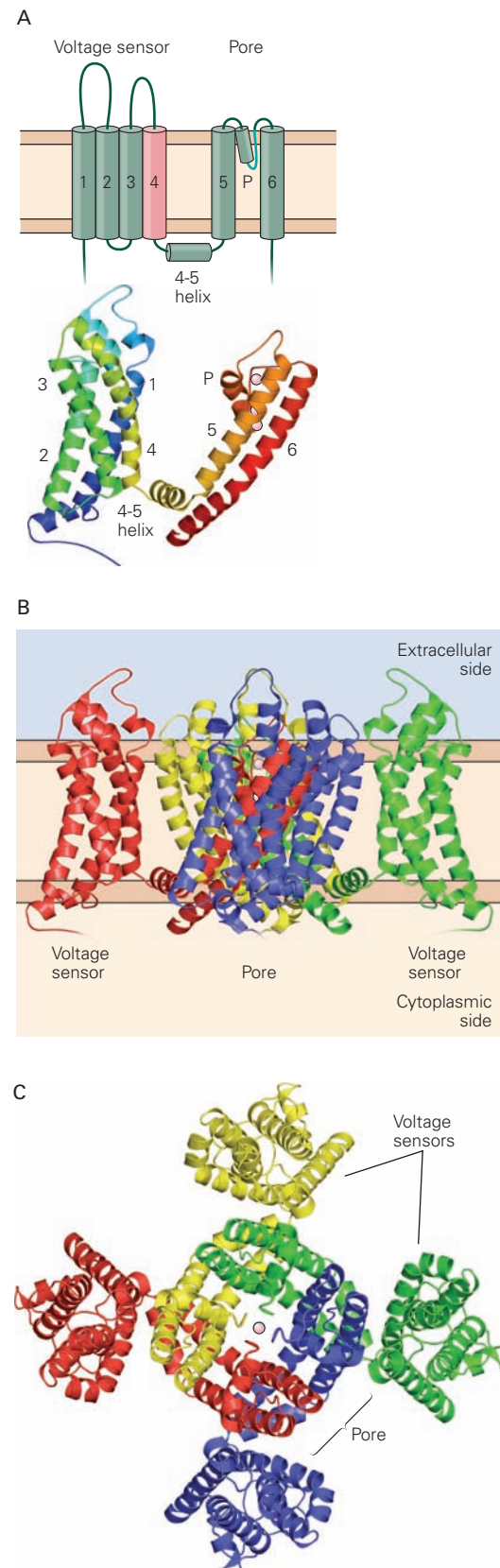


**Figure 7–15** X-ray crystal structure of a voltage-gated  $\text{K}^+$  channel. (Adapted, with permission, from Long et al. 2007.)

**A. Top:** In addition to its six transmembrane  $\alpha$ -helices (S1–S6), a voltage-gated  $\text{K}^+$  channel subunit contains a short  $\alpha$ -helix (the P helix) that is part of the P-region selectivity filter, as well as an  $\alpha$ -helix on the cytoplasmic side of the membrane that connects transmembrane helices S4 and S5 (4-5).

**Bottom:** An X-ray structural model of a single subunit shows the positions of the six membrane-spanning helices, the P helix, and the 4-5 linker helix. Note how the S1–S4 voltage-sensing region and S5–P–S6 pore-forming region are localized in separate domains. Two potassium ions bound in the pore are shown in pink.

**B.** Side view of the tetrameric voltage-gated  $\text{K}^+$  channel. Each individual subunit is highlighted in a different color. The red subunit is in the same orientation as the subunit shown above in panel A. The approximate position of the lipid bilayer is indicated (tan colors).

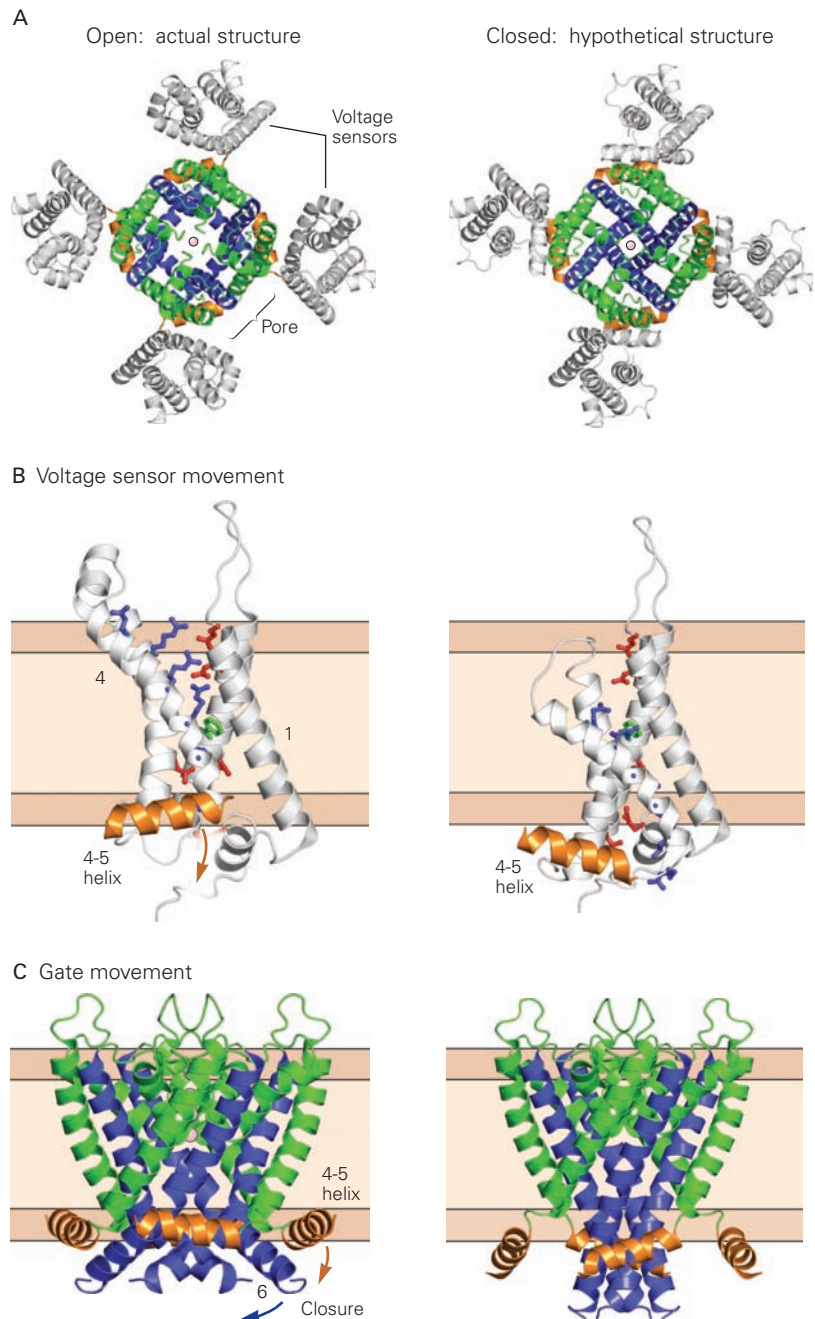
**C.** A view looking down on the tetrameric channel from outside the cell. The four voltage-sensors (S1–S4) are located on the periphery and the S5–P–S6 pore-forming region of the channel is in the center. A potassium ion is shown in the center of the pore (pink). (Adapted, with permission, from Long et al. 2007.)

**Figure 7-16** Model for voltage-gating based on X-ray crystal structures of two  $K^+$  channels. The drawings on the left show the actual structure of an open voltage-gated  $K^+$  channel (from the crystal structure shown in Figure 7-15). The drawings on the right show the hypothetical structure of a closed voltage-gated  $K^+$  channel, based in part on the structure of the pore region of the two-transmembrane segment bacterial  $K^+$  channel KcsA in the closed state. (Adapted, with permission, by Yu-hang Chen from Long et al. 2007.)

**A.** A view looking down on the open and closed channel from outside the cell. Note how the central pore is constricted in the closed state. This constriction prevents  $K^+$  flow through the channel.

**B.** A view of the S1–S4 voltage-sensing domain from the side, parallel to the plane of the membrane. Positively charged residues in S4 are shown as **blue sticks**. In the open state, when the membrane is depolarized, four positive charges on the S4 helix are located in the external half of the membrane, facing the external solution. The positive charges in the interior of the membrane are stabilized by interactions with negatively charged residues in S1 and S2 (**red sticks**). In the closed state, when the membrane potential is negative, the S4 region moves inward so that its positive charges now lie in the inner half of the membrane. The inward movement of S4 causes the cytoplasmic S4–S5 coupling helix to move downward.

**C.** The putative conformational change in the channel pore upon voltage-gating. A side view of the tetrameric S5–P–S6 pore region of the channel shows the S4–S5 coupling helix. Membrane repolarization causes the downward movement of the S4–S5 helix, applying force to the S6 inner helix of the pore. This causes the S6 helix to bend at its glycine hinge, thereby closing the gate of the channel.



As we saw in Chapter 5, the four subunits that comprise the inward-rectifying  $K^+$  channels are truncated versions of the fundamental structural motif; they consist of only the P region and its two flanking membrane-spanning regions. Evolution has provided many of these channels with an extrinsic mechanism of voltage sensitivity through the addition of an internal cationic binding site. When the cell is depolarized,

cytoplasmic  $Mg^{2+}$  or positively charged polyamines (small organic molecules that are normal constituents of the cytoplasm) are electrostatically driven to this binding site from the cytoplasm, plugging the channel.

Inactivation of voltage-gated ion channels is also mediated by different molecular modules. For example, the rapid inactivation of both the A-type  $K^+$  channel and the voltage-gated  $Na^+$  channel is mediated by



a tethered plug that binds to the inner mouth of the channel when the activation gate opens. In the A-type  $K^+$  channel the plug is formed by the cytoplasmic N-terminus of the channel protein, whereas in voltage-gated  $Na^+$  channels it is formed by the cytoplasmic loop connecting domains III and IV of the  $\alpha$ -subunit.

The wide range of firing properties of different neurons and the ability of a single neuron to adapt its firing to a range of synaptic inputs depends on the large diversity of ion channels expressed throughout the nervous system. Even a single ion species, such as  $K^+$ , can cross the membrane through several distinct types of channels, each with its own characteristic

kinetics, voltage dependence, and sensitivity to different modulators. For voltage-gated channels five different mechanisms are responsible for this diversity. (1) More than one gene may encode related  $\alpha$ -subunits within one class of channel. For example, eight different genes that encode voltage-gated  $Na^+$  channel  $\alpha$ -subunits are expressed in the mammalian nervous system. (2) The four  $\alpha$ -subunits that form a  $K^+$  channel may be encoded by different genes. After translation the  $\alpha$ -subunits are in some cases mixed and matched in various combinations, thus forming different subclasses of heteromultimeric channels. (3) A single gene product may be alternatively spliced, resulting in

**Figure 7-17** The extended gene family of voltage-gated channels produces variants of a common molecular design.

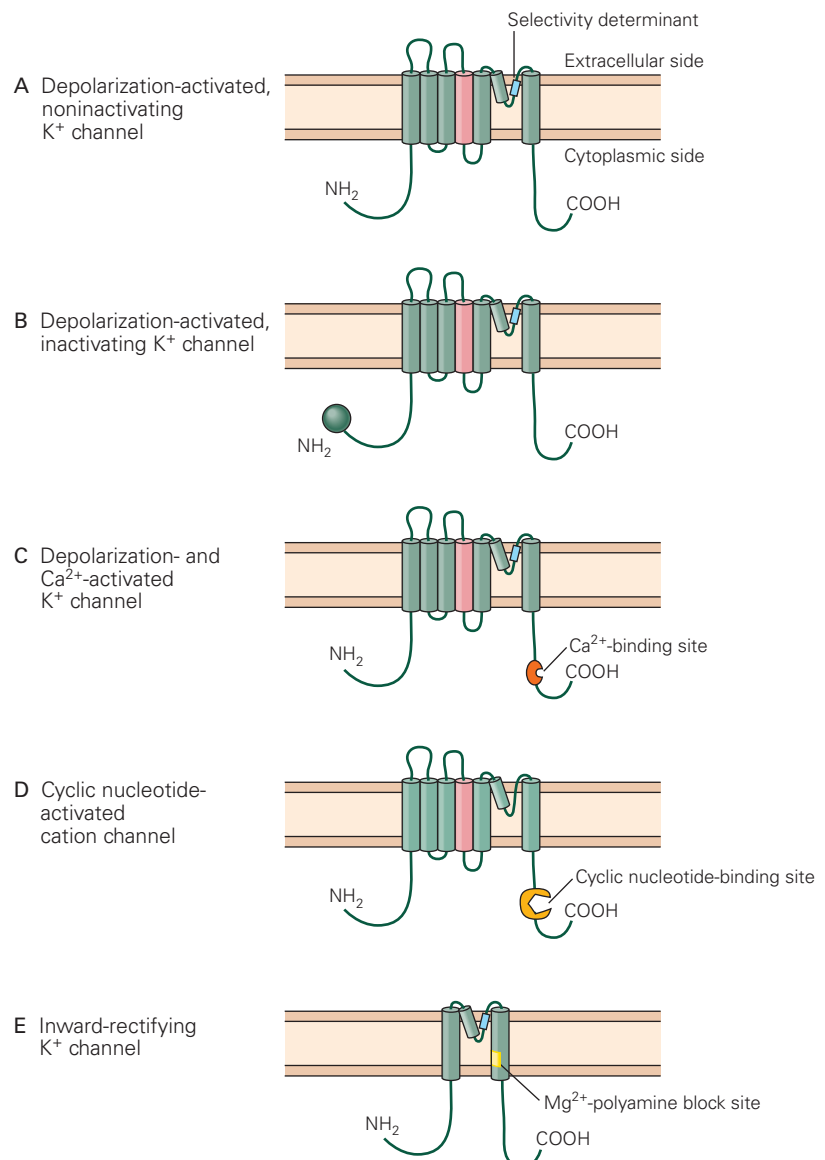
A. The basic transmembrane topology of an  $\alpha$ -subunit of a voltage-gated  $K^+$  channel.

B. Many  $K^+$  channels that are first activated and then inactivated by prolonged depolarization have a ball-and-chain segment at their N-terminal end that inactivates the channel by plugging its inner mouth.

C. Some  $K^+$  channels that require both depolarization and an increase in intracellular  $Ca^{2+}$  to activate have a  $Ca^{2+}$ -binding sequence attached to the C-terminal end of the channel.

D. Cation channels gated by cyclic nucleotides have a cyclic nucleotide-binding domain attached to the C-terminal end. One class of such channels includes the voltage-independent, cyclic nucleotide-gated channels important in the transduction of olfactory and visual sensory signals. Another subclass consists of the hyperpolarization-activated (HCN) channels important for pacemaker activity (see Figure 7-11D). The P loops in these channels lack key amino acid residues required for  $K^+$  selectivity. As a result, these channels do not show a high degree of discrimination between  $Na^+$  and  $K^+$ .

E. Inward-rectifying  $K^+$  channels, which are gated by blocking particles available in the cytoplasm, are formed from a truncated version of the basic building block, with only two membrane-spanning regions and a P-region.





variations in the messenger RNA (mRNA) molecules that encode the  $\alpha$ -subunit. (4) The RNA that encodes an  $\alpha$ -subunit may be edited by chemical modification of a single nucleotide, thereby changing the composition of a single amino acid in the channel subunit. (5) One type of  $\alpha$ -subunit may be combined with different accessory subunits to form functionally different channel types.

These accessory subunits (often termed  $\beta$ -,  $\gamma$ -, or  $\delta$ -subunits) may be either cytoplasmic or membrane-spanning and can produce a wide range of effects on channel function. For example, some  $\beta$ -subunits enhance the efficiency with which the channel is trafficked to the membrane. Other subunits regulate channel gating, either enhancing or inhibiting the coupling of depolarization to channel opening. In some  $K^+$  channels the  $\alpha$ -subunit lacks a tethered inactivation plug; the association of such  $\alpha$ -subunits with  $\beta$ -subunits that contain their own N-terminal tethered plugs can endow the channel with the ability to rapidly inactivate. In contrast to the  $\alpha$ -subunits, there is no known homology among the  $\beta$ -,  $\gamma$ -, and  $\delta$ -subunits from the three major subfamilies of voltage-gated channels.

These various sources of channel diversity also vary widely between different areas of the nervous system, between different types of neurons, and within different subcellular compartments of a given neuron. A corollary of this regional differentiation is that mutations or epigenetic mechanisms that alter voltage-gated channel function can have very selective effects on neuronal or muscular function. The result is a large array of neurological diseases called channelopathies (see Chapter 14).

## An Overall View

An action potential is produced when ions move across the cell membrane through voltage-gated channels and thereby change the charge separation across the membrane. An influx of  $Na^+$ , and in some cases  $Ca^{2+}$ , depolarizes the membrane and initiates the action potential. An efflux of  $K^+$  then repolarizes the membrane by restoring the initial charge separation. A particularly important subset of voltage-gated channels opens primarily when the membrane potential nears the threshold for an action potential; these channels have a profound effect on the spike-train encoding properties of a neuron.

We know much about how channels function from studies that use variations of the voltage-clamp technique—these studies let us eavesdrop on a channel at work. And we know a good deal from biochemical,

molecular biological, and X-ray crystallographic studies about the channel's structure—about the primary amino acid sequence of the proteins that form them and how these proteins adopt their detailed secondary, tertiary, and quaternary structures in the membrane.

Now these two approaches are being combined in a concerted effort to understand the relationship between structure and function in these channels: how the detailed three-dimensional structure of the molecule and the chemical and physical properties of its individual residues gives rise to the remarkable gating and ion permeation properties of the voltage-gated channels. Thus, we may soon be able to understand the molecular mechanism for the remarkable ability of voltage-gated channels to generate the action potential. These insights into channel function have two important practical implications. They will allow us to understand better the molecular bases of certain genetic diseases that involve mutations in ion channel genes, and they will enable us to design safer and more effective drugs to treat a variety of diseases that involve disturbances in electrical signaling (such as epilepsy, multiple sclerosis, myotonia, and ataxia).

---

John Koester  
Steven A. Siegelbaum

## Selected Readings

- Armstrong CM, Hille B. 1998. Voltage-gated ion channels and electrical excitability. *Neuron* 20:371–380.
- Bezanilla F. 2008. How membrane proteins sense voltage. *Nat Rev Mol Cell Biol* 9:323–332.
- Hille B. 2001. *Ion Channels of Excitable Membranes*, 3rd ed. Sunderland, MA: Sinauer.
- Hodgkin AL. 1992. *Chance & Design: Reminiscences of Science in Peace and War*. Cambridge: Cambridge Univ. Press.
- Jan LY, Jan YN. 1997. Cloned potassium channels from eukaryotes and prokaryotes. *Annu Rev Neurosci* 20: 91–123.
- Llinás RR. 1988. The intrinsic electrophysiological properties of mammalian neurons: insights into central nervous system function. *Science* 242:1654–1664.
- MacKinnon R. 2003. Potassium channels. *FEBS Lett* 555:62–65.
- Rudy B, McBain C. 2001. Kv3 channels: voltage-gated  $K^+$  channels designed for high-frequency repetitive firing. *Trends Neurosci* 24:517–526.
- Smart T. 2004. The state of ion channel research in 2004. *Nat Rev Drug Discov* 3:239–278.

Yu FH, Catterall WA. 2003. Overview of the voltage-gated sodium channel family. *Genome Biol* 4(3):207.

## References

- Armstrong CM, Bezanilla F. 1977. Inactivation of the sodium channel. II. Gating current experiments. *J Gen Physiol* 70:567–590.
- Armstrong CM, Gilly WF. 1979. Fast and slow steps in the activation of sodium channels. *J Gen Physiol* 59:388–400.
- Catterall WA. 1988. Structure and function of voltage-sensitive ion channels. *Science* 242:50–61.
- Cole KS, Curtis HJ. 1939. Electric impedance of the squid giant axon during activity. *J Gen Physiol* 22:649–670.
- Dekin MS, Getting PA. 1987. In vitro characterization of neurons in the vertical part of the nucleus tractus solitarius. II. Ionic basis for repetitive firing patterns. *J Neurophysiol* 58:215–229.
- Heinemann SH, Terlau H, Stühmer W, Imoto K, Numa S. 1992. Calcium channel characteristics conferred on the sodium channel by single mutations. *Nature* 356:441–443.
- Hodgkin AL, Huxley AF. 1952. A quantitative description of membrane current and its application to conduction and excitation in nerve. *J Physiol* 117:500–544.
- Hodgkin AL, Katz B. 1949. The effect of sodium ions on the electrical activity of the giant axon of the squid. *J Physiol* 108:37–77.
- Isom LL, DeJongh KS, Catterall WA. 1994. Auxiliary subunits of voltage-gated ion channels. *Neuron* 12:1183–1194.
- Jiang Y, Lee A, Chen J, Ruta V, Cadene M, Chait BT, MacKinnon R. 2003. X-ray structure of a voltage-dependent K<sup>+</sup> channel. *Nature* 423:33–41.
- Jones SW. 1985. Muscarinic and peptidergic excitation of bull-frog sympathetic neurones. *J Physiol* 366:63–87.
- Jones SW, Adams PR. 1987. The M-current and other potassium currents of vertebrate neurons. In: LK Kaczmarek, IB Levitan (eds). *Neuromodulation: The Biological Control of Neuronal Excitability*, pp. 159–178. New York: Oxford Univ. Press.
- Llinás R, Jahnsen H. 1982. Electrophysiology of mammalian thalamic neurones *in vitro*. *Nature* 297:406–408.
- Long SB, Tao X, Campbell EB, MacKinnon R. 2007. Atomic structure of a voltage-dependent K<sup>+</sup> channel in a lipid membrane-like environment. *Nature* 450:376–382.
- McCormick DA, Huguenard JR. 1992. A model of electrophysiological properties of thalamocortical relay neurons. *J Neurophysiol* 68:1384–1400.
- Noda M, Shimizu S, Tanabe T, Takai T, Kayano T, Ikeda T, Takahashi H, et al. 1984. Primary structure of *Electrophorus electricus* sodium channel deduced from cDNA sequence. *Nature* 312:121–127.
- Papazian DM, Schwarz TL, Tempel BL, Jan YN, Jan LY. 1987. Cloning of genomic and complementary DNA from *Shaker*, a putative potassium channel gene from *Drosophila*. *Science* 237:749–753.
- Payandeh J, Scheuer T, Zheng N, Catterall WA. 2011. The crystal structure of a voltage-gated sodium channel. *Nature* 475:353–59.
- Sigworth FJ, Neher E. 1980. Single Na<sup>+</sup> channel currents observed in cultured rat muscle cells. *Nature* 287:447–449.
- Stevens CF. 1991. Making a submicroscopic hole in one. *Nature* 349:657–658.
- Vassilev PM, Scheuer T, Catterall WA. 1988. Identification of an intracellular peptide segment involved in sodium channel inactivation. *Science* 241:1658–1661.
- Yang N, George AL Jr, Horn R. 1996. Molecular basis of charge movement in voltage-gated sodium channels. *Neuron* 16:113–122.